



# Recent advances in slippery liquid-infused surfaces with unique properties inspired by nature

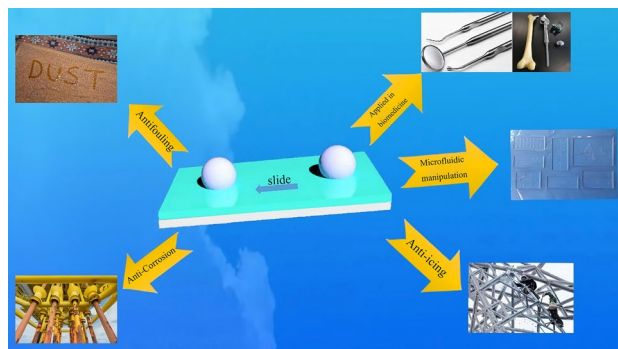
Xi Zeng<sup>1,2</sup> · Zhiguang Guo<sup>1,2</sup> · Weimin Liu<sup>2</sup>

Received: 3 February 2021 / Accepted: 27 March 2021 / Published online: 3 May 2021  
© Zhejiang University Press 2021

## Abstract

The slippery liquid-infused porous surface(s) (SLIPS) that imitates the *Nepenthes* pitcher plant has proven to be highly versatile and can be combined with various surface characteristics such as dynamic response, antifouling, selective adhesion, and optical/mechanical tunability. In addition, the introduction of a lubricating fluid layer also gives it extremely low contact angle hysteresis and self-repairing properties, which further expands its application range. Currently, SLIPS has been proven to be suitable for many frontier fields such as aerospace, communications, biomedicine, and microfluidic manipulation. In this review, we explain the theoretical background of SLIPS and the preparation methods currently available, including the choice of substrate materials and lubricants, and we discuss the design parameters of the liquid injection surface and how to deal with the consumption of lubricants in practical applications. In addition, the paper focuses on current and potential applications, such as preventing pathogen contamination and blood adhesion of medical equipment, manipulation of tiny droplets, and directional transportation of liquids. Finally, some weaknesses that appear when SLIPS is used in these applications are pointed out, which provides a new perspective for the development of SLIPS in the future.

## Graphic abstract



**Keywords** SLIPS · Lubricant-infused · Slippery · Repellent surface · Preparation · Application

✉ Zhiguang Guo  
zguo@licp.cas.cn

<sup>1</sup> MOE Key Laboratory of Green Preparation and Application for Functional Materials, Hubei University, Wuhan 430062, China

<sup>2</sup> State Key Laboratory of Solid Lubrication, Lanzhou Institute of Chemical Physics, Chinese Academy of Sciences, Lanzhou 730000, China

## Introduction

Various phenomena in nature give us inspiration for design and creation. Organisms with special wettability are common in nature, such as lotus leaves [1], rice leaves [2], and cicada wings [3], which exhibit strong hydrophobicity. With the development of surface science and micro-/nanomanufacturing technology, it has been discovered that superhydrophobicity is closely related to surface energy and surface roughness.

Surface energy is determined by the chemical composition of a surface, and surfaces are usually rendered hydrophobic by a certain amount of roughness. By imitating the microstructure of these biological surfaces, it is possible to prepare artificial surfaces that also have superhydrophobicity. In recent decades, a large number of studies have been conducted on superhydrophobic surfaces. Bionic surfaces with special wettability have gradually penetrated into all aspects of our lives, including antifouling for hygiene and sanitation [4–10], anti-ice and anticorrosion in the transportation industry [11–16], anti-thrombosis and bacterial adhesion in the medical field [17–22]. In the process of continuous exploration, more and more deficiencies have gradually been exposed. For example, it is difficult to repel organic liquids and other low-surface-tension contaminants for anti-fouling [23]. When used for anti-icing, performance will fail in high-humidity environments [24]. In the medical field, even if it can repel blood, the surface can still adhere to proteins and cause pollution [25]. In addition, poor mechanical stability is a common problem of most superhydrophobic surfaces. Structural defects are prone to cause loss of function after wear or shearing. Therefore, in order to overcome these deficiencies, a new repellent surface called slippery liquid-infused porous surface(s) (SLIPS) has been developed. Inspired by the *Nepenthes* pitcher plant, a lubricant is infused into a porous base material to produce a thin liquid film on the surface [23]. The lubricant is usually an oily or ionic liquid with low surface tension, to achieve liquid–liquid rather than liquid–solid interface repulsion. In addition, the repellence of the interface prevents direct contact between solids and the base material and prolongs the service life of the repelling surface. In this review, we describe the theoretical basis for SLIPS design and the methods of preparation. In addition, we discuss the preparation process of SLIPS from the aspect of materials, including the types of substrate materials and the choice of lubricants. Next, special attention is paid to ways of dealing with lubricant consumption in practical application. Also outlined are current and potential areas of interest for application and the latest findings, including some deficiencies in these applications. Finally, we provide a new perspective on the future of SLIPS research and propose directions for research development.

## Theoretical foundation and background

### Theoretical foundation

The concept of wettability was first proposed by Thomas Young in the early nineteenth century. He discovered a specific angle formed when liquid contacts a solid surface in air, which is now called the contact angle [26]. When a droplet contacts a solid surface in a state of mechanical equilibrium,

the contact angle's value can be calculated by Young's equation [27]:

$$\cos\theta = \frac{\gamma_{sv} - \gamma_{sl}}{\gamma_{lv}},$$

where  $\theta$  is the value of static contact angle (CA).  $\gamma_{sv}$ ,  $\gamma_{sl}$ , and  $\gamma_{lv}$  represent the solid–vapor, solid–liquid, and liquid–vapor interfacial tensions, respectively (Figs. 1a and 1b). Young found that a liquid contact angle increases as the surface becomes more repellent [28]. When the value of the static contact angle of water is  $0^\circ \leq \theta \leq 90^\circ$ , the water droplet can spread on the surface and the surface is referred to as hydrophilic, but when the angle is  $90^\circ < \theta \leq 180^\circ$ , the surface not be wetted by water and is called hydrophobic. According to Young's equation, a contact angle of  $90^\circ$  is the threshold between hydrophobicity and hydrophilicity [28]. Young's equation is used to calculate the contact angle on the flat surface, but in fact there is no ideal flat surface, and all kinds of surfaces are often uneven even if only at the atomic level. Consequently, in 1936, Wenzel modified Young's equation and introduced the roughness factor ( $r$ ) [29]:

$$\cos\theta = r \cdot \cos\theta_0 = r \cdot \frac{\gamma_{sv} - \gamma_{sl}}{\gamma_{lv}},$$

$r$  is the ratio of the actual rough surface area to the projected area.  $\theta_0$  is Young's contact angle of the liquid droplet on a flat substrate (see Figs. 1c and 1d). Wenzel indicated that wetting is the process of replacing the solid–gas interface area with a solid–liquid interface of the same area, usually accompanied by the extension of the liquid–gas interface [30]. Since each interface has its specific surface energy content, when the wettability process occurs, the total surface energy will increase or decrease as the range of each interface changes. Therefore, wetting is a thermodynamic process. Whether wetting occurs or not depends on the change of free energy. The greater the change, the greater the possibility of wetting and the higher the degree of wetting. Conversely, the smaller the change in free energy, the smaller the ability to overcome wetting resistance, making wetting difficult to achieve. For smooth and hydrophobic surfaces, the surface energy of the material and the corresponding surface tension are lower. According to Young's equation, the contact angle of the liquid surface is greater than  $90^\circ$  on this type of surface and the droplets are often spherical. In the process of replacing the solid–air interface with the solid–liquid interface, the area of solid–liquid contact increases, resulting in greater changes in free energy; so the water repellency of the solid surface increases, causing both the contact angle of the droplet on the solid surface and the sphericity of the droplet to increase [31].

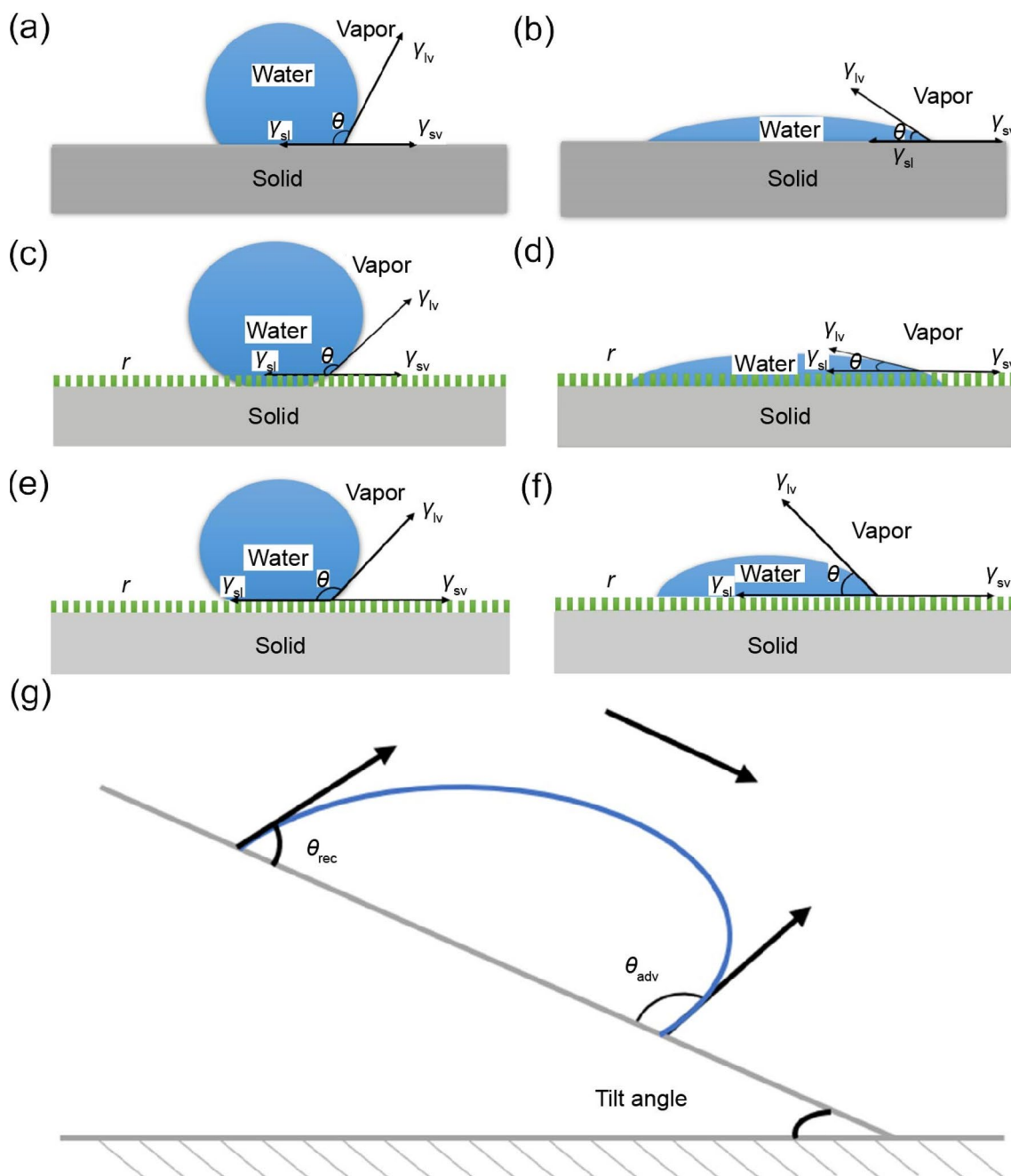


**Fig. 1** Hydrophobic (a) and hydrophilic (b) wetting state of water droplets on a smooth surface (Young's model). The hydrophobic (c) and hydrophilic (d) wetting state from the Wenzel model. The hydro-

phobic (e) and hydrophilic (f) wetting state from the Cassie-Baxter model. g The contact angle hysteresis of the droplet on the inclined surface

Wenzel's equation was originally designed to reveal the wetting mechanism of a liquid with a single uniform solid surface. If the composition of a rough solid surface is not uniform, it is composed of two or more different substances. In order to calculate the contact angle of such composite interfaces, the Wenzel equation is further modified. Taking a two-component composite interface as an example, the

contact angle of a liquid at this interface can be calculated using the following formula [32]:

$$\cos\theta = f_1\cos\theta_1 + f_2\cos\theta_2,$$

where  $f_1$  and  $f_2$  are the percentages of the total area in contact with the liquid composed by components 1 and 2.  $\theta_1$  and  $\theta_2$  are the corresponding intrinsic contact angles of a liquid

droplet on the two materials, and this is the famous Cassie–Baxter equation [33].

When the solid–liquid interface replaces the solid–air interface, the voids on the rough surface may not be completely filled with liquid (see Figs. 1e and 1f). A solid–liquid–air composite interface is formed. In this case, there is a layer of air between the liquid and the solid because the liquid is not in contact with the solid surface. In order to calculate the contact angle of the composite interface in this case, the contribution of the fractional area of wet surfaces and the fractional area with air pockets is combined and the Cassie–Baxter equation can be expressed as [34]:

$$\cos\theta = r \cdot \cos\theta_0 - f_{LA} \cdot (r \cdot \cos\theta_0 + 1),$$

where  $\theta_0$  is the contact angle for a smooth surface of the solid material,  $r$  is the roughness factor, and  $f_{LA}$  is the fractional flat geometric area of the liquid–air interfaces under the droplet. According to the above formula, even if a solid surface is hydrophilic, as the value of  $f_{LA}$  gradually increases to a sufficiently large value, the surface can still be changed from hydrophilic to hydrophobic. In fact, this is only a theoretical inference. In practical situations,  $f_{LA}$  may not increase all the way to the critical value of hydrophilic–hydrophobic transition, or when it increases to this value, the solid–liquid contact state deviates from the Cassie–Baxter model. Therefore, the critical conditions for the hydrophilic–hydrophobic transition can be obtained according to this formula [29]:

$$f_{LA} \geq \frac{r \cdot \cos\theta_0}{r \cdot \cos\theta_0 + 1}.$$

At this point, the value of  $\theta_0$  is less than  $90^\circ$ .

### Contact angle hysteresis

In studying surface wetting behavior, the contact angle hysteresis  $\theta_H$  is a very important data point [29]. It is essentially an indicator to measure the energy loss during droplet flow along a solid surface. This energy loss is caused by surface roughness and unevenness. When the droplet is on an inclined surface and simply slides downward due to the influence of gravity, the downward contact angle is called the advancing contact angle ( $\theta_{adv}$ ), and the upward angle is called the receding contact angle ( $\theta_{rec}$ ) (see Fig. 1g). Research shows that the advancing angle is linked to surface wettability and the receding angle to surface adhesion [28]. Generally,  $\theta_{adv}$  is larger than  $\theta_{rec}$ , and the value of contact angle hysteresis is determined by the difference between  $\theta_{adv}$  and  $\theta_{rec}$ :

$$\theta_H = \theta_{adv} - \theta_{rec}.$$

In summary, Young’s equation, Wenzel’s equation, and the Cassie–Baxter model describe the static wettability of

a solid surface, while the dynamic wettability of a system is described by the advancing angle, receding angle, and contact angle hysteresis.

### Types of water-repellent materials

The oldest fossils found to date were from Western Australia. These fossils are similar to today’s cyanobacteria and are about 3.5 billion years old. Therefore, we can conclude that the origin of life was no later than 3.5 billion years ago. Over such a long period of time, the environment is constantly changing and organisms are constantly adapting to the natural environment through evolution. Therefore, a series of special wettability surfaces naturally arose. The most well known is the lotus leaf surface, where water droplets tend to be spherical and roll easily without leaving traces [35–37]. It is well known that the water-based properties of lotus leaves are due to the network of waxy crystals on the surface and the nanostructures on the top of the microscale nipples [29, 35] (see Fig. 2a). Therefore, by imitating the microstructure of the special wetted surface of lotus leaves and other biological examples, scientists have prepared a variety of bionic surfaces with unusual wettability that can play an important role in different environments. Superhydrophobic surfaces like imitation lotus leaf can be used for anti-fouling, anti-icing, and other applications [29]. Imitation fish scales with a super hydrophilic/underwater super-oleophobic surface can be used for low-cost oil transportation and oil–water separation, reducing both the cost of offshore oil extraction and oil leakage during the extraction process [34, 38, 39] (see Fig. 2b). Imitation alternate hydrophilic and hydrophobic surfaces modeled on desert beetles can be used for water collection, alleviating the shortage of water resources in arid areas [40–42] (see Fig. 2c). More recently, inspired by the *Nepenthes* pitcher plant, a hydrophobic surface with an ultralow sliding angle was prepared [23, 43] which can be used in medical equipment [17], microfluid delivery, and corrosion prevention in the marine industry [44, 45] (see Fig. 2d).

### Slippery liquid-infused porous surface(s) (SLIPS)

*Nepenthes* is a carnivorous plant that lives in tropical areas. It has highly specialized leaves adapted to attract, capture, retain, and digest arthropod prey. It is based on special surface properties of the pitcher rim (peristome) and insect “aqua planing.” The peristome is characterized by a regular microstructure with radial ridges of smooth overlapping epidermal cells, which form a series of steps toward the pitcher inside and make it superhydrophilic. This superhydrophilic surface can be completely wetted by rain in humid weather,

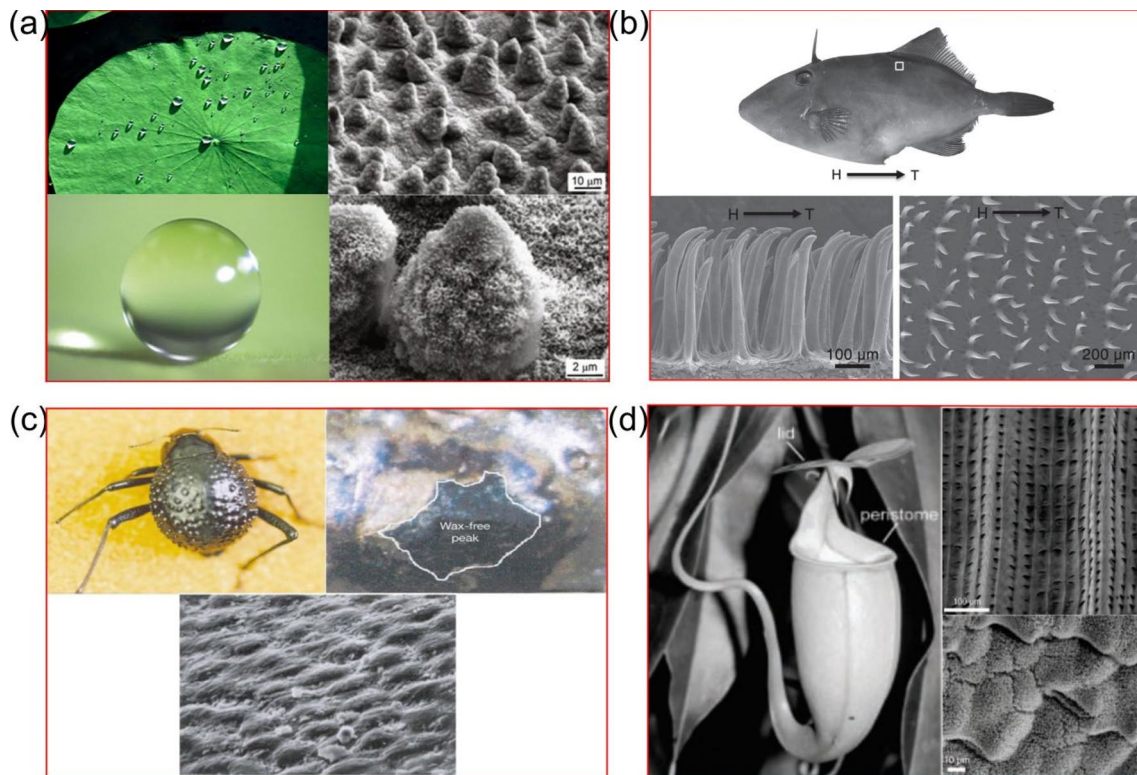


**Fig. 2** **a** Optical photograph and scanning electron microscope (SEM) image of lotus leaf. Reproduced with permission [29]. Copyright 2009, The Royal Society. **b** Optical photograph of filefish *N. septentrionalis* and SEM image of its back skin. Arrows H to T indicate the direction from head to tail. Reproduced with permission [39].

Copyright 2014, Wiley–VCH Verlag. **c** Picture of desert beetle and back SEM image. Reproduced with permission [40]. Copyright 2001, Nature Publishing Group. **d** Photograph of *Nepenthes* pitcher plant and SEM image of the inner wall of the insect trap. Reproduced with permission [43]. Copyright 2004, Natl Acad Sciences

so that a uniform liquid film covers the surface. The flower then releases a special fragrance to attract insects to step on the peristome surface, which repels the oil on their feet to make them slide down from the edge into the digestive juices at the bottom. Inspired by *Nepenthes*, the researchers combined the roughness of the microstructure with well-matched solid and liquid surface energies. The porous micro-/nano-structure of the substrate, in combination with chemical adsorption, allows the introduced lubricant to form a more stable combination with the substrate and spread evenly to form a liquid film on the surface. This surface is called slippery liquid-infused porous surface(s) (SLIPS). Generally, the lubricant and the repelled liquid are not compatible with each other, and the surface tension is much lower than that of the repelled liquid in order to induce repulsion, which naturally occurs between liquids of different polarities. Unlike Cassie state systems, the lubricant in the SLIPS system prevents direct contact between the bottom solid material and the test liquid and effectively prevents the problem of the test liquid potentially damaging the structure of the solid surface and causing the performance of the superhydrophobic surface to fail. Moreover, this liquid-infused system is very slippery and pressure stable, making it capable of handling

low surface tension liquids, providing optical transparency, and self-healing after mechanical damage.

### Preparation of SLIPS

SLIPS is composed of two parts: a substrate and a lubricant. Therefore, SLIPS is usually prepared in two steps; the first step is to design a superhydrophobic substrate, and the next is to add an infused lubricant. It is common knowledge that for superhydrophobic surfaces, surface roughness, surface free energy, and uniformity of chemical composition are three important factors that affect wettability [46, 47]. However, in SLIPS, the influence of the first two factors is more significant due to the existence of the surface liquid layer. Generally, when preparing SLIPS, a low-surface-energy substrate with a textured structure is selected, or a surface with a rough structure is modified by an appropriate chemical coating to make it more suitable for lubricant infusion [48, 49]. At present, most studies use a combination of two methods to obtain the substrate, because a stable SLIPS is more dependent on the combination of the lubricant and the substrate rather than the roughness of the substrate, even though in general, surfaces with a rough structure have a

better ability to retain lubricant than smooth surfaces [49, 50]. In addition, a variety of methods can be used to obtain a textured surface, including chemical etching [51, 52], plasma etching [53], photolithography [54–56], anodic oxidation [57, 58], crystal growth [59], electrodeposition [60], and electrospinning [61–63]. Of these, photolithography has high repeatability and can accurately control the geometry of the introduced surface structure. Even though the process is complex and requires specialized equipment, photolithography is still the most effective method for constructing reentrant structures.

## Substrate

In order to prepare a liquid-infused system, a porous template needs to be strategically designed so that the lubricant will not escape from the substrate [46]. Different materials are chosen as substrates according to the situation, and the concept of liquid-infused surfaces has already been applied to numerous materials [64]. Currently, the materials used as SLIPS substrates can be roughly divided into three categories: metals, inorganic nonmetallic materials, and porous polymers.

### Metals

The footprint of metal materials is ubiquitous in all industries. Therefore, it is of practical significance to give metal materials better surface properties. Designing SLIPS on metal materials can give them extra performance. For example, in dairy industrial processing, SLIPS can be used to prevent the growth of fouling on the surface of industrial equipment during dairy product heat treatment; food-grade stainless steel is prepared as a substrate, via femtosecond laser ablation, followed by fluorosilanization and impregnation with an inert perfluorinated oil product. Titanium is often used as a bioreplacement material, such as in joint replacement and dental implants [64, 65]. Although titanium has been proven to be biofilm-repellent and can inhibit bacterial colonization, there is still a bacterial biofilm-induced risk of microbial infection, and as a result, titanium-based SLIPS has attracted attention. Doll et al. [65] used a femtosecond laser system to impart surface roughness to the titanium substrate and then infused perfluoropolyether lubricant to prepare SLIPS that had strong repellency to biofilms. Leyla Soleymani's research group used chemical vapor deposition to create self-assembled monolayers of fluorosilane on gold-modified prestrained polystyrene substrates [66]. After heat shrinking of the substrate, a lubricant is applied to produce a lubricant-infused wrinkled nanostructured gold surface with hydrophobic properties (see Fig. 3a). In addition to being hydrophobic, this surface has a contact angle of about 150° on the surface and a sliding angle of less than

5°. It has good self-cleaning properties. In terms of anti-biological adhesion, it reduces blood protein adhesion and significantly prolongs blood clotting time [66]. It is important to note that a layer of metal on the surface makes the surface conductive yet still resistant to bio-adhesion, which is the basis for using SLIPS in the fields of biosensing and medical equipment. In addition, Yang's team used the electrodeposition method to prepare a porous silver membrane surface with strong wettability, switching ability, and liquid repellency [60] (see Fig. 3b). With silver nitrate and sodium dodecyl sulfate (SDS) as the electrolyte, the wettability switch and liquid repellent performance are achieved by the dodecyl sulfate ions ionically bonded to the porous membranes during electrodeposition. Dodecyl chain tails are inherently hydrophobic. When a negative potential is added, dodecyl chain tails will hide in the surface of the porous silver membrane, making the overall system superhydrophilic. When this superhydrophilic surface is exposed to organic reagents, due to the strong affinity of dodecyl chain tails for organic reagents, they will be stretched out from the porous silver membrane, making the surface superhydrophobic, thus achieving wetting state transition from super hydrophilic to superhydrophobic. After negative potential is added to the system again, it will immediately become superhydrophilic, and the cycle of changing the applied conditions to adjust the wettability state can be repeated more than ten times without significant degradation (see Figs. 3c and 3d). Depending on the need to adjust the injected lubricant to achieve hydrophobic or oleophobic properties, this technique can be applied in various applications, including encryption, controllable droplet transfer, and water harvesting. Other metal substrates that have been reported so far are aluminum, stainless steel [67–70], carbon steel [71, 72], gold [66], Co [73], and Mg [74, 75].

### Nonmetallic materials

With the advancement of manufacturing and technology, especially the development of inorganic chemistry and organic chemical industries, natural or synthetic nonmetallic materials have received increasing attention. Although nonmetallic materials have poor electrical and thermal conductivity, they can be used as substitutes for metals in some fields and are an indispensable part of the current chemical industry. Therefore, in the preparation of SLIPS, research on nonmetallic materials as substrates has been continuously reported, for example wood, glass, and silicon [76]. Guo et al. added a ZnO nanorod array on a wooden surface to obtain a micro-/nanostructure, and then functionally modified the surface with 1H, 1H, 2H, 2H-perfluorooctyltriethoxysilane (PTES) to make it superhydrophobic. Finally, a fluorinated lubricant was infused to generate an omniphobic wood surface which repelled arbitrary liquids (aqueous

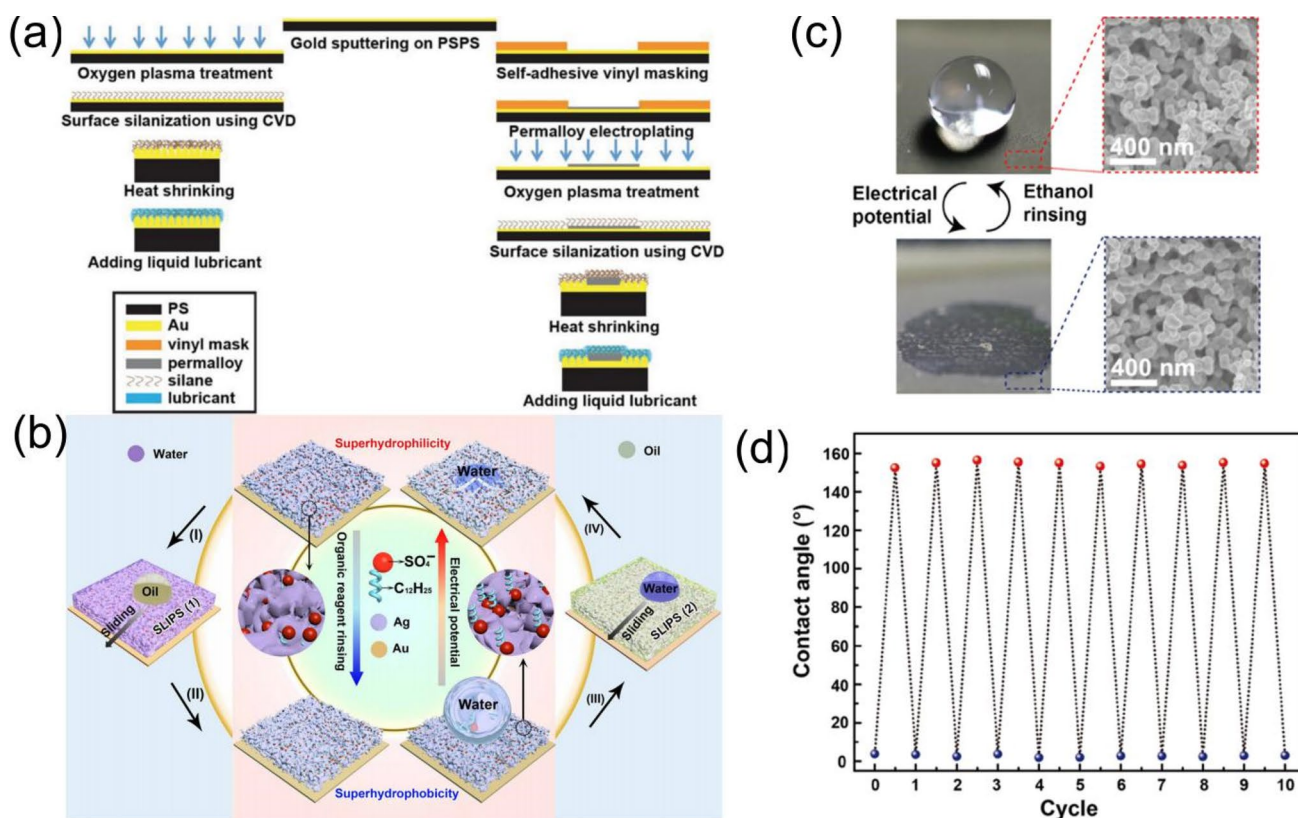


**Fig. 3** **a** Schematic diagram of preparation process for a conductive lubricant to be injected into the surface of the nanostructure. Reproduced with permission [66]. Copyright 2018, John Wiley and Sons Ltd. **b** Liquid repellency and reversible wettability transition of the silver porous film surface. **c** After ten wettability transitions, the sur-

face morphology of the silver porous membrane has not changed. **d** Contact angle of water on the surface of the silver porous membrane when the wettability is periodically switched. Reproduced with permission [60]. Copyright 2019, Royal Soc

or organic) [77] (see Figs. 4a–4c). Since the wooden surface exhibits a unique surface pattern on the predetermined microscale of the natural cell structure, it has groove-like channels and cell walls when longitudinal ridges are cut. Therefore, using this natural surface microstructure combined with additional nanostructures, one can achieve a surface with complex properties and reduced manufacturing costs. The wooden surface itself and the array of ZnO nanorods are highly porous, so they can effectively capture the liquid lubricant. The obtained omniphobic surface shows extremely low wettability to water or oil (see Fig. 4d). Shen's [78] working group treated a wood surface with sandpaper to obtain a rough surface, then cast and dried a fluoroalkylsilane/silica composite suspension on the surface to produce superhydrophobicity, improving the water resistance and mildew resistance of the wood (see Figs. 4e–4h). After cyclic wear under a pressure of 3.5 kPa for 45 cycles, the surface still maintained superhydrophobicity. Even if the superhydrophobicity is damaged, the performance can be restored by recasting the fluoroalkylsilane/silica composite suspension at normal temperature. Silicon has definite non-metallic properties, and silicon and its organic compounds

also have excellent properties such as low surface tension, resistance to high and low temperatures, oxidation stability, and corrosion resistance. Varanasi et al. obtained silicon microparticles by patterning silicon substrates with photolithography [18]. The column array was modified with a low-surface-energy silane to give it a functionalized surface, and immersed in lubricant, finally, remove the excess lubricant, and the team explored the contact line morphology of water droplets and lubricant. Rather than exhibiting fundamentally different behaviors, these distinct morphologies not only govern the contact line pinning that controls droplets' initial resistance to movement but also the level of viscous dissipation and hence their sliding velocity once the droplets begin to move. Kim et al. used the emulsion template method to prepare self-stratifying porous silicones (SPS) with closed-cell porosity. This method allowed water droplets near the surface to evaporate and eventually disappear during the curing process, creating a nonporous skin layer [79]. The internal void structure was formed by the evaporation of water droplets accumulated before the polymer was completely solidified. After that, the silicone oil was infused as a lubricant, and the liquid-infused system was complete. The

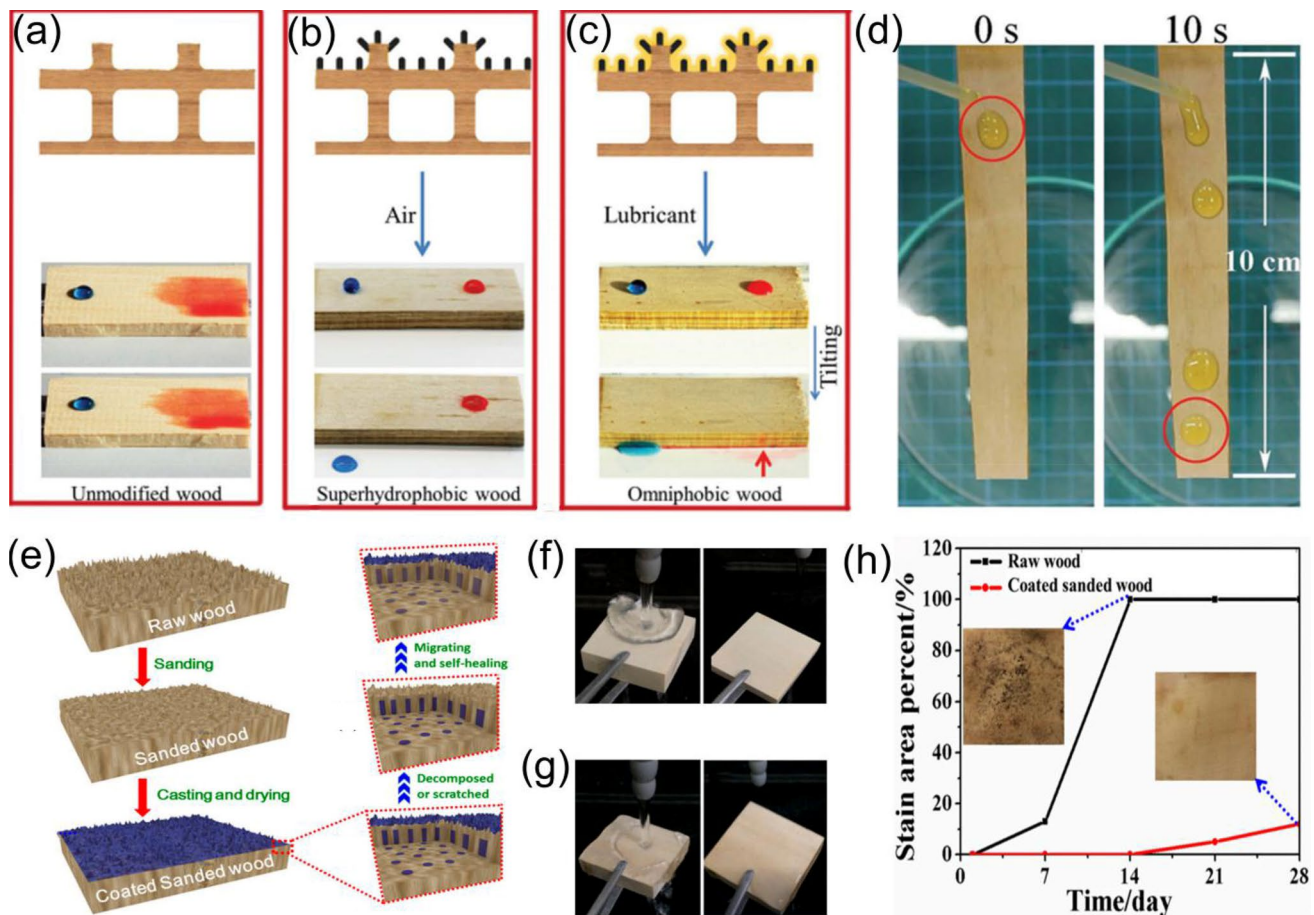


**Fig. 4** **a** Original wood surface without surface modification. **b** ZnO nanorod array is added to the wood surface and functional modification is performed. **c** Lubricant is infused after adding ZnO nanorod array and performing functional modification. Note: The test droplets are water (blue) colored with methylene blue and hexadecane (red) colored with Aero-Brite dye. **d** The olive oil slides on the lubricant-infused surface. Reproduced with permission [77]. Copyright 2017,

John Wiley and Sons Ltd. **e** Schematic diagram of the preparation process. **f** and **g** are the comparison diagrams of the superhydrophobic surface and the original surface before and after water washing. **h** Comparison of mold infections on two surfaces in a humid environment. Reproduced with permission [78]. Copyright 2020, MDPI (Basel, Switzerland)

emulsion template method can change the porosity, pore size distribution, and thickness of the nonporous skin layer of SPS by adjusting the concentration of water and surfactant in the precursor emulsion, as shown in Fig. 5. Compared with nonporous polydimethylsiloxane (PDMS), SPS has better lubricant injectability and ability to lock in lubricant, which improves the stability of the entire liquid-infused system.

### Porous polymer

Because of their excellent toughness properties and easy adjustment to different shapes and sizes, porous polymers are very popular for preparing slippery liquid-infused porous surfaces. Currently reported are polyvinyl chloride, polycarbonate, polytetrafluoroethylene (PTFE) [79], poly(methyl methacrylate), PDMS [17, 80], and polystyrene (PS), among others. The first liquid-infused porous surface designed by

Aizenberg et al. tried to use periodically ordered and random arrays of nanoposts functionalized with a low-surface energy polyfluoroalkyl silane and a random network of Teflon nanofibers as the substrate. Chen et al. used a one-step femtosecond laser direct writing method to directly generate a connected three-dimensional porous network microstructure on a polyamide-6 (PA6) substrate [81] (see Fig. 6a). On this basis, SLIPS was prepared by further modification and infused lubricant, which has good self-healing properties. The sliding angle of various liquids on this surface is about  $10^\circ$ . Because PA6 is an inherently antiwear material and there is a certain cushioning effect of the lubricant layer on the surface, the maximum bending angle after wear is about  $180^\circ$ , as shown in Fig. 6b. Moreover, the sliding angle of the water droplets was still less than  $3^\circ$  when the wear cycle reached 100 times, demonstrating that the surface has good durability (see Fig. 6c). It has also been reported that a

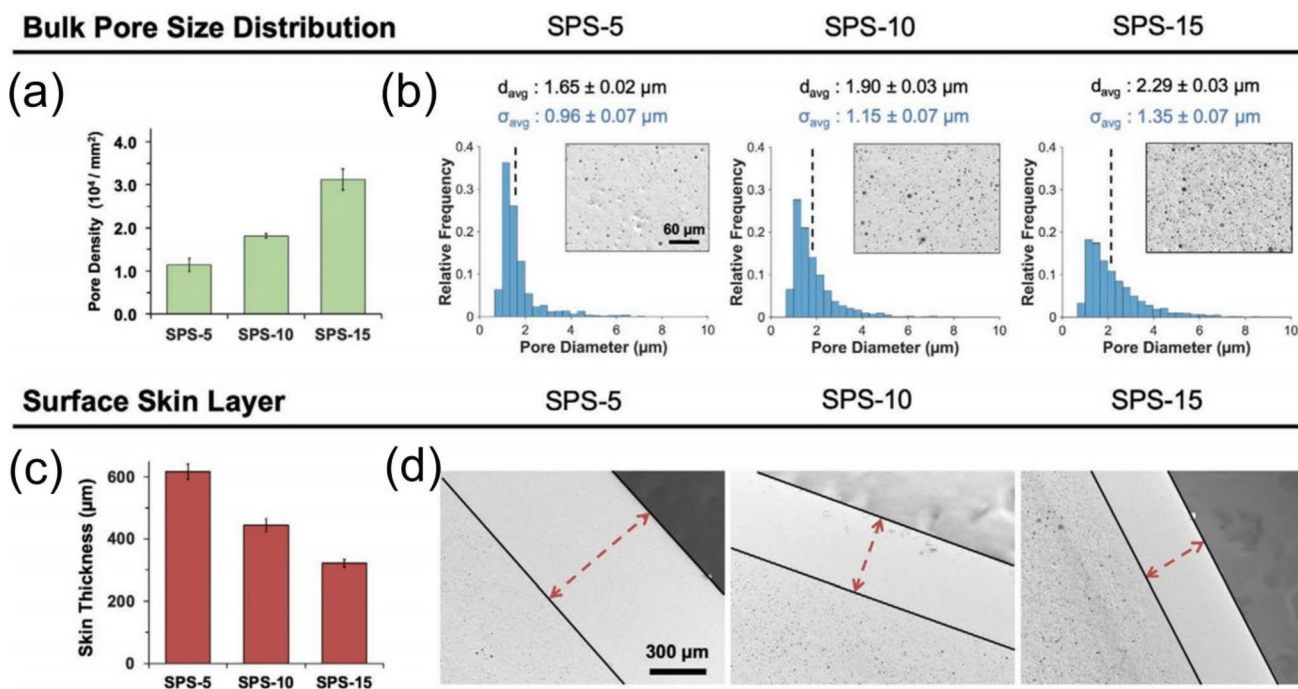


**Fig. 5** SPS-5, SPS-10, and SPS-15 indicate the use of different concentrations of precursors to prepare SPS samples; the concentration increases as the number increases. **a** and **b**, respectively, represent the

contrast of pore density and pore size distribution. **c**, **d** Comparison of surface liquid layer thickness. Reproduced with permission [79]. Copyright 2020, John Wiley and Sons Ltd

fluorinated polymer monomer based on cross-linked hydroxyethyl methacrylate (HE) can be infused into perfluoropolyether to produce SLIPS [82]. This liquid-infused system was

designed by Oleschuk et al. [83]; they successfully added paramagnetic particles to the test liquid and then drove it by magnetic force. In liquid-phase chemical synthesis, a small

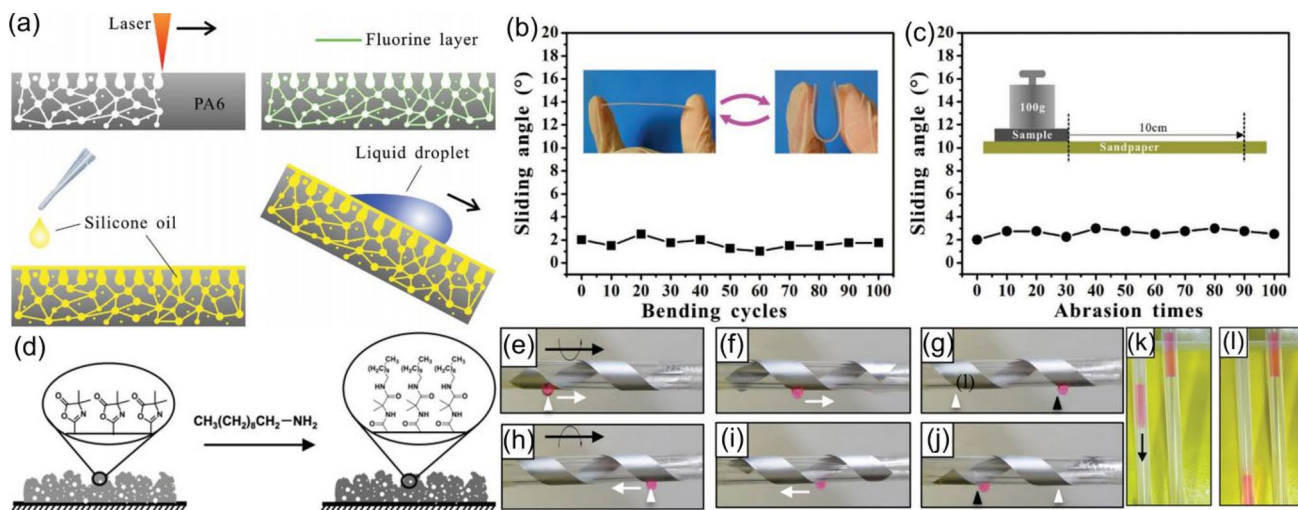


**Fig. 6** **a** Simplified schematic diagram of SLIPS prepared by femto-second laser. **b** The value of the sliding angle when cyclically bending SLIPS. **c** The changing trend of the sliding angle as the amount of wear increases. The test liquid in (b) and (c) is deionized water. Reproduced with permission [81]. Copyright 2017, John Wiley and Sons Ltd. **d** Post-fabrication functionalization of residual azlactone groups in nanoporous PEI/PVDMA multilayers by reaction with

*n*-decylamine. **e–g** SLIPS rotating counterclockwise controls the lateral transfer of water droplets. **h–j** SLIPS rotating clockwise controls the lateral transfer of water droplets. **k**, **l** SLIPS-coated flexible PTFE tubing (left) and tubing without an SLIPS coating (right). The inclination angle is about 3  $^\circ$ . Reproduced with permission [82]. Copyright 2015, Wiley-Blackwell

volume of liquid is more affected by viscosity than inertia, and the reaction is more precise and rapid, which improves the product yield. This microfluidic technology can be used in on-chip polymer synthesis and liquid–liquid extraction. They tested the contact angles and sliding angles of five kinds of normal alkanes (hexane, heptane, octane, tetradecane, and hexadecane) and five alcohols (methanol, ethanol, 1-decanol, cyclohexanol, and ethylene glycol) with water. The surface tensions of the liquids were quite different, and their sliding angles on the synovial fluid injection system were all between 4° and 6°. In the process of magnetic driving, whether the liquid could be successfully driven was related to the concentration of paramagnetic particles and the acceleration rate of the magnet. Lynn et al. [82] designed a polymer multilayer film that could manufacture physically and chemically stable SLIPS on objects of any shape, size, or topology, making it suitable for bending and folding (see Figs. 6e–6l). They chose azlactone-functionalized multilayers fabricated using poly(vinyl-4,4-dimethylazlactone) (PVDMA) and branched poly(ethyleneimine) (PEI), because PEI/PVDMA multilayers are covalently cross-linked, and they have strong physical and chemical stability. Simultaneously, the remaining azlactone in the film can be treated by strategically selected amine-functionalized molecules to adjust the surface wettability to meet the response requirements (see Fig. 6d). Finally, silicone oil is injected into the porous multilayer polymer prepared on the flat glass to obtain a stable lubricating liquid-infused system which can repel a variety of liquids, including acid/alkaline solutions, ketchup, and serum-containing cell culture medium. When dripping the silicone oil onto the surface, the sliding angle on the injected SLIPS is approximately 6°.

## Lubricant

Selection of the lubricant is an important step in the preparation of SLIPS. A lubricant compatible with the substrate can improve the stability of the entire liquid-infused system. In this section, we will explain some lubricants to contribute to designing a more perfect SLIPS. The performance of liquid-infused porous surfaces depends on a stable surface liquid layer to drive out water or other contaminants and protect the material [79]. The stability of SLIPS is not only related to the properties, types, and surface micro-/nanostructure of the substrate, but also to the physical and chemical properties of the lubricant itself. Caitlin et al. [84] explored the relationship between the amount of lubricant loss on the surface in a flowing environment and the microstructure of the substrate and type of lubricant. They prepared mesofluidic channels with flat and structured fluorinated surfaces in order to visualize lubricant loss and provide confirmation of the results found using the peristaltic pump. Two different viscosity lubricants (Krytox 103 and perfluorodecalin) were infused

into two mesofluidic channels, and the results showed that with the increase in the channel flow rate, there was a slight difference in the loss of lubricant; thus, the loss of lubricant with lower viscosity was relatively higher. Therefore, an appropriate choice of lubricants is one of the most important steps in the design of SLIPS. The choice of lubricant should be considered from two aspects: the balance between the lubricant and the base, and between the lubricant and the test liquid. Wong et al. gave three criteria for synthesizing SLIPS: (1) the lubricating fluid must be moist and adhere to the inside of the substrate stably. (2) The substrates must be wetted by the lubricating fluid first, not the test fluid. (3) The test fluid and the lubricating fluid must be incompatible with each other. From a thermodynamic point of view, in order to ensure that the substrate is preferentially wetted by the lubricating fluid, the interface energy between the fluid, the lubricating fluid, and the base material should satisfy the following equation [23]:

$$\Delta E_1 = r \cdot (\gamma_2 \cos \theta_2 - \gamma_1 \cos \theta_1) - \gamma_{12} > 0,$$

$$\Delta E_2 = r \cdot (\gamma_2 \cos \theta_2 - \gamma_1 \cos \theta_1) + \gamma_1 - \gamma_2 > 0$$

where  $E_1$  and  $E_2$  are the energy of the lubricating fluid with or without a fully wetted immiscible test liquid floating on top of it,  $\gamma_1$  and  $\gamma_2$  are the surface tensions of the test fluid and the wetting fluid, respectively,  $\gamma_{12}$  is the interfacial tension at the liquid–liquid interface,  $\theta_1$  and  $\theta_2$  are the equilibrium contact angles of the immiscible test liquid and the lubricating fluid on a flat solid surface, and  $r$  is the roughness factor [85].

The second criterion is to select lubricants with specific properties according to different application environments. For example, for devices that require optical transparency, it is necessary to match the refractive index between the lubricant and the substrate. For applications that require long-term stability or involve elevated temperatures, a more viscous oil can be selected. These oils tend to have low vapor pressures and high boiling points. In addition, fluorine-free hydrophobic lubricants (such as silicone oil or hydrocarbon oil) can be used for water solvents. Likewise, polar lubricants can be used to repel low-surface-tension hydrocarbons, allowing a wider variety of lubricants [28]. Due to its outstanding features in anti-fouling, anticorrosion, and self-repair applications, liquid-infused surfaces have attracted widespread attention in recent years. Commonly used infused lubricants include Krytox oils, hydrocarbon silicone oils, mineral oil, and ionic liquids. There have been an increasing number of studies on the slippery liquid-infused porous surface, but these studies are more focused on the type of substrate, the morphology, and the wide range of use of the liquid-infused system, and the impact of the lubricant during use has been relatively little explored. The common means of lubricant loss are diffusion

to the surrounding surface, external shear, and the influence of gravity or evaporation [77, 86]. However, the repellency of SLIPS has an important relationship with the lubricant, and the loss of the lubricant may cause the loss of SLIPS function. The current research offers two main approaches to dealing with this loss of lubricant. One is to enhance the bond strength between the lubricant and the substrate by strengthening the chemical interaction and capillary phenomenon, slowing down the loss of the lubricant. This can be understood as liquid retention, and it is generally applied to any surface. The second approach is to design an interconnected porous structure in the base material which can store the liquid. When the surface lubricant is lost, the internally stored liquid replenishes the surface liquid layer through the connected pore structure to maintain repulsion performance, a process known as liquid restoration. Tian et al. [87] believe that to deal with high-temperature evaporation of lubricants, one can either choose a fluid with a low evaporation rate, or add a compound to the lubricant to reduce the vapor pressure through the strong interaction after mixing. Therefore, they designed a fluid composed of self-suspended nanoparticles capped by perfluorinated ligands to improve the lubricant evaporation performance of SLIPS. By adding  $\text{Fe}_3\text{O}_4$  nanoparticles to the perfluorinated fluid to form a mixture, they can greatly reduce the evaporation loss of the lubricant when the temperature is higher than room temperature. The result is shown in Fig. 7a, and the self-suspended nanoparticles capped by perfluorinated ligands showed negligible evaporation over more than 100 days at temperatures up to 50 °C. When the temperature reached 90 °C, the evaporation rate was more than 50% lower than that of perfluorinated ligand without nanoparticles. Zhang et al. [88] reported a UV-responsive slippery surface based on silicone oil and a porous silicon-based substrate containing azobenzene groups. Since the substrate has a porous network structure, the lubricant and the substrate also have good chemical affinity. Therefore, a large amount of silicone oil is retained on the surface of the substrate and the porous network structure inside (see Fig. 7b). When the lubricant layer on the surface is lost, due to the conformational transformation of the azobenzene groups under UV light irradiation, the lubricant lost from the surface could be self-replenished, eventually rebuilding a new lubricant layer to reform the slippery surface. The conformational change of the azobenzene groups causes the substrate to shrink slightly, and the silicone oil stored inside is squeezed and released to the surface to form a new lubricant layer to restore slippery performance. It has been proved that this kind of SLIPS can repeatedly restore the surface lubricant layer, exhibiting good chemical and physical stability under a variety of difficult environments and significantly improving the service life of SLIPS (see Figs. 7c–7f). In addition, Deng et al. [89] imitated the lubrication mechanism of earthworms and designed a liquid

releasable polymer coating to introduce a texture structure. The lubricating oil forms a randomly distributed embedded block structure in the polymer substrate. Even if the lubricating oil layer on the surface is lost, it will be quickly released to the surface under external mechanical stimulation to restore the original smooth surface.

## Application

### Antifouling

A variety of self-cleaning materials have been developed for daily life, industry, the military, and other fields [48]. The superhydrophobic self-cleaning surface stimulated by the “lotus leaf effect” is one of them. The surface wax layer and multiscale microstructures work together to cause a high contact angle and a low sliding angle. The water droplets are spherical on the lotus leaf, so they can easily roll in any direction, and dirt particles are also easily removed. However, the limited ability to resist oily pollutants hinders its practical application to a certain extent [23]. SLIPS has a low surface friction coefficient and a very low sliding angle [90]. Compared with superhydrophobic surfaces, the sliding angle is usually less than 5°. Although it is well known that the rolling of water droplets is more conducive to removing pollutants than sliding, the mechanical stability and omniphobic properties of SLIPS confer more advantages. Therefore, slippery liquid-infused porous surfaces have broad prospects for antifouling. For example, in the food processing industry, pollution is a common problem that requires a large amount of water and energy for sanitation, and the significant impact on the environment does not meet the requirements of current social development. In response to the growth of dirt on the stainless-steel walls of industrial equipment in the dairy processing industry, Jimenez et al. [67] designed a lubricant-infused surface on food-grade stainless steel. The texture structure is introduced into the stainless-steel substrate by femtosecond laser etching, and then the inert perfluorinated oil is infused after modification by fluorosilane. The contact angle hysteresis of the obtained SLIPS is only 0.6°, providing superhigh sliding properties. Lei et al. [90] designed an SLIPS based on porous poly-high internal phase emulsion (HIPE) membrane with good antifouling properties. When using silicone oil with low surface tension as the injection liquid, the sliding angle of water droplets on this poly HIPE-based SLIPS film is about 3° and can easily repel oil-based pollutants such as ink, coffee, and milk (see Figs. 8a and 8b). In addition, it has good resistance to solid pollutants such as dust. The liquid-infused slippery surface designed by Dong et al. [71] on carbon steel can remove  $\text{Fe}_3\text{O}_4$  powder with

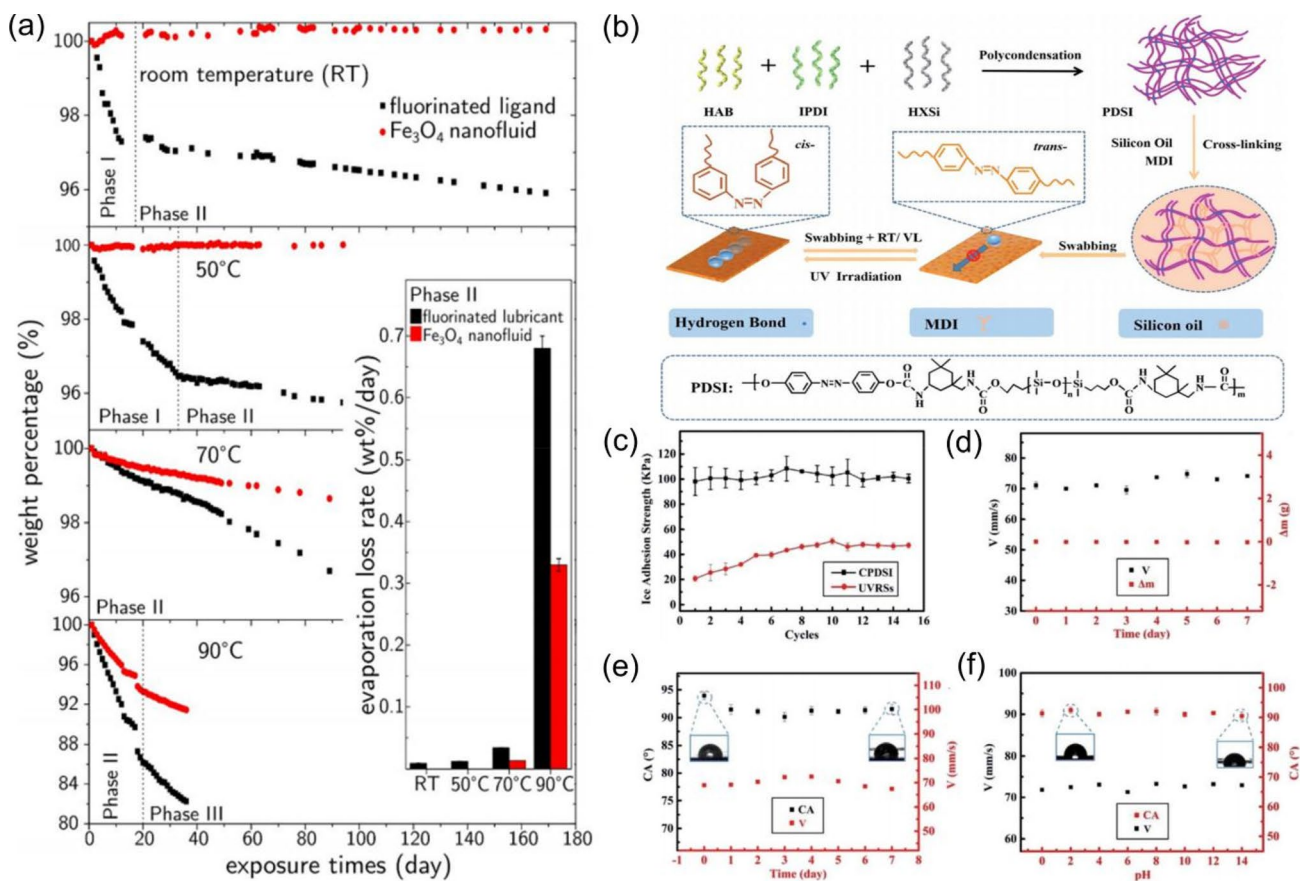


**Fig. 7** a SLIPS prepared with fluorinated ligands and Fe<sub>3</sub>O<sub>4</sub> nanofluids, showing the percentage of lubricant mass loss caused by evaporation at different temperatures. The red color represents Fe<sub>3</sub>O<sub>4</sub> nanofluid and the black color represents fluorinated ligand. Reproduced with permission [87]. Copyright 2020, ACS. b The preparation procedure and UV-responsive behavior of UVRSSs (RT: room temperature; VL: visible light). c The change in ice adhesion strength as the

number of cycles between CPDSI and UVRSSs increases. d The sliding velocity and mass change after UVRSS is immersed in water and then rotated at a speed of 200 r/min. e Changes in contact angle and sliding velocity when UVRSS is maintained at 80 °C with increasing time. f Sliding velocity and contact angle of liquids with different pH values on UVRSS. Reproduced with permission [88]. Copyright 2020, Royal Society of Chemistry

sliding water droplets (see Figs. 8c and 8d). Guo et al. [91] used ultraviolet light to graft polydimethylsiloxane onto ZnO nanorods and then infused silicone oil to prepare a lubricant-fixed slippery surface. This slippery surface is not only resistant to common liquids in daily life such as water, ketchup, and honey (see Fig. 8e), but after being boiled for 15 min, the water droplets can still slide at an inclination angle of 4°. After soaking in strong acid/alkali solution for 400 h, the surface still exhibits excellent slippery stability. This liquid-infused slippery surface, which can withstand harsh environments and remain stable, has huge practical application potential. We believe that anti-fouling with superhydrophobic surfaces is an inevitable choice for the continued development and progress of human society.

### Anti-icing

The problem of ice accumulation has always been unavoidable in life and industry, especially for equipment that is exposed to the natural environment year-round, such as high-voltage power lines, railroad tracks, airplanes and ships, and communication facilities [24, 92–96]. Ice accumulation can cause damage to equipment, interfere with its normal operation, and increase maintenance costs. The use of human resources or mechanical deicing equipment is expensive and inefficient, but these were the only options before superhydrophobic surfaces were developed. Studies have found that icing is significantly delayed when water is on a superhydrophobic surface [97]. This is because the contact area between water droplets and the surface is reduced, resulting in a decrease in the nucleation center of ice crystals. However, the freezing of water on a superhydrophobic surface is

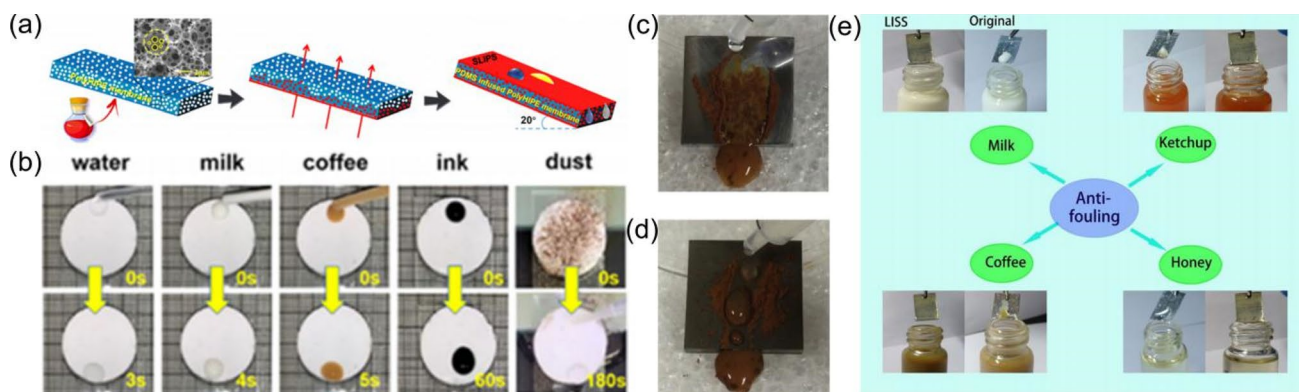


**Fig. 8** **a** PDMS-infused poly (high-internal-phase emulsion) templates for the construction of slippery liquid-infused porous surfaces. **b** Repelling a series of liquid and solid pollutants. Reproduced with permission [90]. Copyright 2019, ACS. **c**, **d** Self-cleaning test of basic steel (upside) and sliding surface (downside) with an inclina-

tion angle of  $15^\circ$  with  $\text{Fe}_3\text{O}_4$  solid particles as pollutants. Reproduced with permission [71]. Copyright 2019, Elsevier. **e** Resistance to a series of common liquids. Reproduced with permission [91]. Copyright 2019, Royal Society of Chemistry

a complicated phenomenon [48]. It not only depends on the water repellency of the surface, but on the particle size of the exposed rough structure. Jung's research shows that the surface of nanoscale particles close to the critical nucleation radius has better ice resistance [98]. At the same time, the environment may also greatly change freezing performance. For example, under high-humidity conditions, a superhydrophobic surface cannot resist icing [24, 99]. SLIPS provides a slippery and chemically uniform surface and may eliminate the nucleation center whether on the surface or on the edge [98], effectively reducing ice formation and adhesion under high-humidity conditions [93]. Aizenberg et al. [93] developed an SLIPS prepared on an aluminum surface (see Fig. 9a), which not only effectively removes surface ice/frost condensation, but also has ice adhesion that is at least an order of magnitude lower than other materials. They used the electrodeposition method to deposit corrosion-resistant highly textured polypyrrole (PPy) on the aluminum substrate and then injected lubricant to meet the SLIPS standard after fluorination modification. Compared to the untreated aluminum surface, the contact angle hysteresis is significantly reduced. In addition, the aluminum-based SLIPS still has good ice resistance under environmental conditions of up to 60% humidity (see Figs. 9b–9f). Later, they explored the effect of SLIPS on the nucleation of supercooled water and designed SLIPS based on an aluminum pan [100]. Compared with untreated aluminum and superhydrophobic surfaces that freeze under high-humidity conditions, SLIPS has the lowest nucleation temperature, and it remains stable after 150 freeze–thaw cycles. Juuti et al. [101] also designed a slippery liquid-infused surface with good ice adhesion resistance on  $\text{TiO}_2$  nanoparticles (see Fig. 9g). The adhesion strength of ice is measured by centrifugal force, and the ice is separated from the surface under the action of centrifugal

force (see Fig. 9h). The results show that the ice adhesion strength of SLIPS is as low as 12 kPa, and the ice resistance performance is significantly better than other surfaces. After multiple ice adhesion cycles, performance was still undiminished. Similarly, the SLIPS prepared by Long et al. on magnesium alloy with a spraying method also showed better ice resistance than superhydrophobic surfaces (SHS) [102] (see Fig. 9i). The ice adhesion strength is expressed by the pulling force required to pull three different surfaces (bare Mg sheet, SHS, SLIPS) out of the ice surface, and the results show that the tensile force required to pull off the surface without lubrication is about six times that required for SLIPS (see Figs. 9j and 9k). After multiple refrigeration cycles, the sliding angle of SLIPS still remained at a low level (see Fig. 9l). As an anti-icing surface, SLIPS has a variety of excellent properties, but there are still some problems to be solved. Regardless of the purpose, the service life and efficiency are not negligible factors in practical applications. Preventing loss of lubrication during the deicing process and eliminating edge ice nucleation is a promising direction for future research.

## Biomedical applications

Biofilm adhesion and blood adhesion are unavoidable problems in medical equipment use and medical implants. Biological fouling of medical devices may cause blood clot formation, pathogen adhesion growth, or implant fibrosis [21, 25, 103]. The medical approach to preventing these devices from causing thrombosis and pathogen contamination is the use of blood thinning drugs and antibiotics. However, these medications may cause excessive bleeding and pathogen resistance, so it is preferable to solve the problem of biofilm adhesion from the device side. SLIPS provides materials

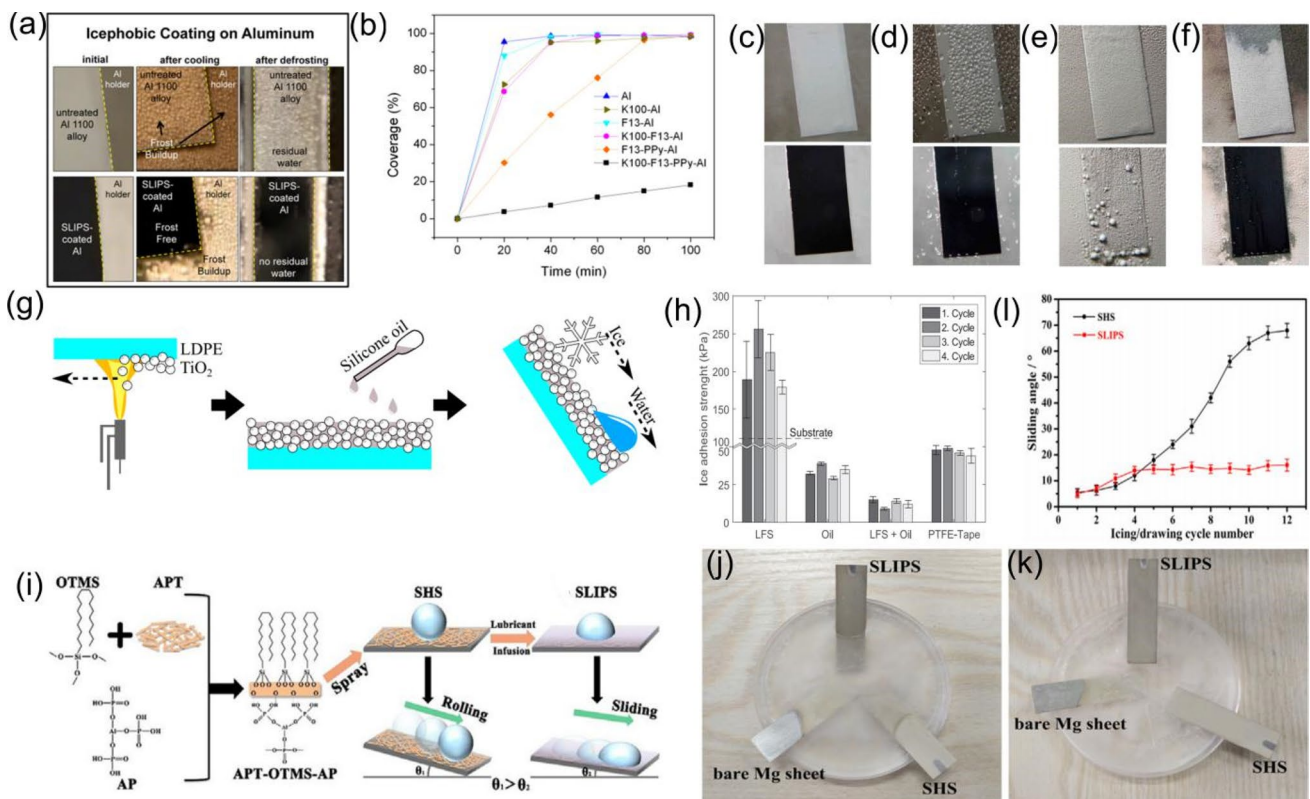


**Fig. 9** **a** Aluminum with anti-icing coating. **b** Fraction of the surface covered by ice on large aluminum samples as a function of cooling time at  $-2\text{ }^{\circ}\text{C}$  and at 60% humidity. **c–f** Representative photographs of Al (top) and SLIPS-Al (bottom) under high-humidity conditions: initial, cooling, frozen, and heating. Reproduced with permission [93]. Copyright 2012, ACS. **g** Schematic diagram of the preparation of SLIPS on LDPE. **h** Measurement results of surface ice adhesion

strength on four surfaces. Reproduced with permission [101]. Copyright 2017, American Institute of Physics. **i** Schematic diagram of the process of preparing SLIPS on magnesium alloy. **j** Frozen photos. **k** Photograph of pulling three kinds of surfaces out of the ice. **l** Changes in the sliding angle between SLIPS and the surface without lubricating fluid after multiple refrigeration cycles. Reproduced with permission [102]. Copyright 2020, Elsevier

with the ability to resist most biological fluids and has great potential in biomedical applications [25]. Leslie et al. [104] added perfluorodecalin (LP) to tethered perfluorocarbon (TP) to form a smooth liquid film layer to resist biofilm adhesion, effectively resist blood and blood components, and prevent bacterial adhesion. Furthermore, they suggested that this smooth liquid film coating can be used on almost any medical-grade material surface. Similarly, Yin et al. [105] prepared a lubricant-infused surface by injecting fluorocarbon liquid into a fluorocarbon-tethered wrinkling surface to resist the adhesion of bacteria and blood, in turn preventing protein adhesion (see Figs. 10a and 10b). In addition, compared to poly(styrene-*b* isobutylene-*b* styrene) (SIBS) references, the adhesion amount of *E. coli* and *Staphylococcus aureus* after 24 h of incubation decreased by about 98.8% and 96.9%, respectively (see Figs. 10c and 10d). However, blindly resisting adhesion also seems to have a negative impact in certain applications that rely on targeted adhesion [106, 107]. Didar et al. [106] reported a lubricant-infused surface that can resist adhesion of biological fluids while promoting targeted binding of desired antibodies. A

chemical vapor deposition (CVD) method is used to prepare self-assembled monolayers (SAMs) of a mixture of 3-aminopropyltriethoxysilane (APTES) and trichloro(1H,1H,2H,2H-perfluorooctyl)silane (TPFS), and then a lubricant is infused to form lubricant-infused surfaces (see Fig. 10e). This slippery surface not only has the characteristic of resisting biological fluids, but by changing the mixing ratio of the two materials, the adhesion degree of the cells that need to be targeted for binding can be adjusted. This is a major breakthrough for the use of biosensors and bioimplants. Zou et al. [108] proposed a composite patch film with anisotropic surface wettability and adhesion in order to enhance tissue repair after surgical treatment. This composite membrane is composed of an anti-adhesive SLIPS and a sticky hydrogel surface, which can quickly induce cell adhesion and growth while avoiding any adhesion to adjacent visceral tissues (see Fig. 10f). It is widely reported that the use of SLIPS-based coatings on medical devices can prevent the growth of pathogens. In fact, this is not accurate. This method has certain limitations. Even if pathogens are not attached to the surface of medical equipment, they can still spread in

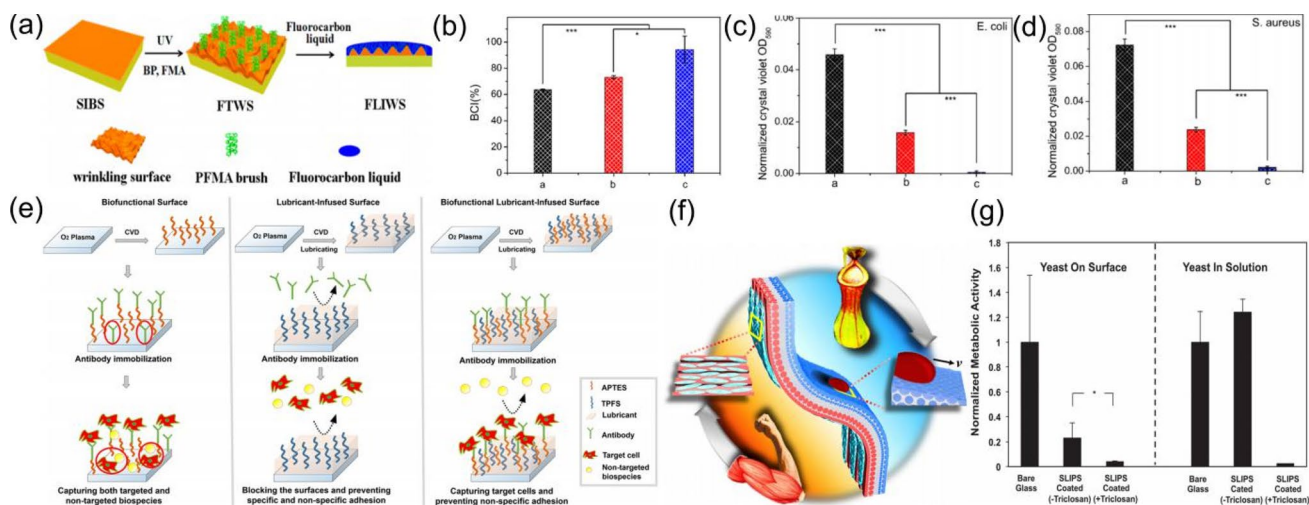


**Fig. 10** **a** Fabrication of a fluorocarbon liquid-infused wrinkling surface. **b** Blood coagulation index of three kinds of surfaces. Among them, black represents SIBS, red represents fluorocarbon-tethered wrinkling surface (FTWS), and blue represents fluorocarbon liquid-infused wrinkling surface (FLIWS). A higher blood coagulation index means that the surface has better antithrombotic properties. **c** Crystal violet staining-based quantification of adherent *E. coli* after incubation for 24 h. **d** Crystal violet staining-based quantification of adherent *S. aureus* after incubation for 24 h. Reproduced with permission [105]. Copyright 2015, ACS. **e** Using chemical vapor depo-

sition or a liquid deposition method creates a schematic diagram of the biofunctional lubricant injected into the surface. Reproduced with permission [106]. Copyright 2018, ACS. **f** Schematic diagram of composite patch film. Reproduced with permission [108]. Copyright 2020, ELSEVIER. **g** The metabolic activity of *Candida albicans* on the surface of bare glass, SLIPS-coated glass, and SLIPS-coated glass with triclosan (left) and the activity of planktonic yeast growing in the surrounding medium (right). Reproduced with permission [22]. Copyright 2016, Wiley–VCH Verlag

nearby human tissues. Palecek et al. [22] reported a multi-functional slippery surface that not only prevents adhesion, but also inhibits the proliferation of surrounding pathogens. Additionally, they injected an antibacterial agent into the nanoporous polymer, which can kill bacteria as the lubricant is released to the surroundings. Like other SLIPS reported, it can greatly reduce the adhesion of bacteria on the surface, and has a significant inhibitory effect on *C. albicans* after the addition of antibacterial agents (Fig. 10g). This method further expands the scope of application of SLIPS in the medical field. Finally, SLIPS seems to offer a perfect solution for resisting the adhesion of biofilms, yet there are still some problems that require more in-depth thinking and further research, such as whether SLIPS can completely prevent thrombosis and bacterial adhesion, whether it can maintain good stability within the organism, whether it will affect the growth of healthy cells while inhibiting the growth of bacteria, and whether the injected lubricant has issues such as toxicity.

## Microfluidic manipulation

Traditional methods of manipulating continuous microfluidics usually require liquids to be contained in microchannels and then controlled by pumps and valves [109]. These devices are not only expensive and complicated, but also, the movement of liquids is limited by the length of the channels.

Droplet-based microfluidic manipulation can be applied in the fields of biology, chemistry, and medical analysis. This discrete droplet transfer can be performed without complicated channels and power equipment, and is a reliable way to achieve the same effect. The commonly used methods of driving droplets are surface acoustic wave [110], static electricity, magnetism, and thermal polarization [111]. The movement of droplets on a solid surface is related to the pinning of the contact line caused by the contact angle hysteresis. Reducing the solid–liquid contact area can reduce the pinning of the contact line. SLIPS can produce a surface liquid layer that causes smaller contact angle hysteresis, so they can greatly enhance the application potential of microfluidic manipulation of droplets. Fu et al. [110] used a surface acoustic wave (SAW) method to drive droplets on SLIPS (Figs. 11a–11c). In order to ensure that the droplets can be successfully driven, the thickness of the lubricant layer is designed to be much smaller than the wavelength of the ultrasonic wave to reduce the ultrasonic resistance of the liquid layer. This method of using SAW to drive droplets can move them stably along the ultrasonic propagation path and is superior because of its low cost and good repeatability. The phase change based on the lubricant can also adjust the movement of the droplets on SLIPS. Chen et al. [112] injected paraffin wax into the olivine crystal thin film of the orderly assembled silica (SiO<sub>2</sub>) nanoparticles and found that the prepared SLIPS could control the movement

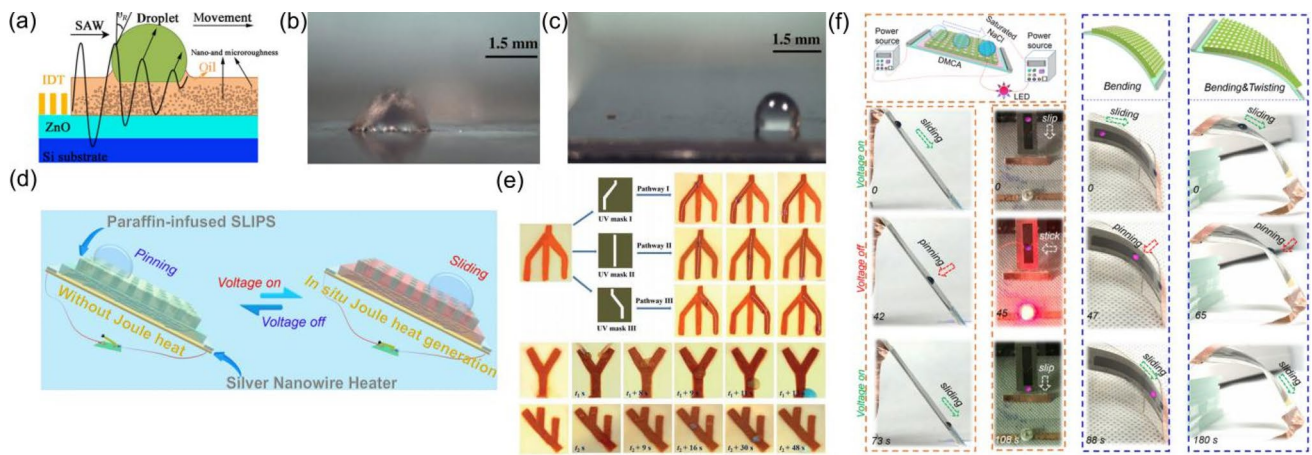


**Fig. 11** **a** Schematic diagram of the interaction between SAW and droplets on the surface of SLIPS. **b** 2  $\mu\text{l}$  DI water is applied to the surface without silicone oil injection. **c** The surface injected with silicone oil at an SAW power of 0.19 s. Reproduced with permission [110]. Copyright 2017, American Physical Society. **d** Schematic

diagram of paraffin-infused SLIPS combined with silver nanowires. **e** Dynamic control of droplet movement on CUVRS with three complex channels. **f** In situ reversible droplet control between pinning and sliding on multidimensional surfaces. Reproduced with permission [113]. Copyright 2019, ACS

of the droplets. The conversion of paraffin wax between solid phase and liquid phase is adjusted by electric heating. When the DC power supply is connected, the paraffin on the conductive path melts, and the droplet will move along the path. As long as the conductive path is changed, the droplet movement path can be flexibly controlled. Li et al. [113] also reported a study of a lubricant phase change to guide the movement of droplets. Paraffin was infused into the zinc oxide film of a micropillar array and combined with a silver nanowire heater (Fig. 11d). With a connected DC power supply, the droplets become movable from the pinning due to the melting paraffin. This method can be used to manipulate the moving path of droplets on a complex three-dimensional surface, and it has good circulation capabilities (Fig. 11f). The transition of surface wettability can also be used to complete the movement of droplets. Zhang et al. [88] designed a smart UV-responsive SLIPS in which silicone oil is infused into a porous silicon substrate containing azobenzene groups. Under ultraviolet light with a wavelength of 365 nm, the azobenzene groups undergo a conformational transformation and lose the lubricant to change the wetting behavior. Therefore, the path of the droplet movement can be manipulated by changing the pattern of the UV mask to achieve complex droplet migration. In addition, the color of the illuminated part will also change, and the pattern of the path and the route of the droplet can be predicted clearly. This new method advances the application of SLIPS in liquid manipulation and microfluidics (Fig. 11e). In addition to the abovementioned methods, manipulation of droplet movement by introducing electric potential to change wettability or magnetism has also been reported [66, 83, 114, 115]. The application of droplet-based microfluidic manipulation in the

fields of chemistry, biology, and medical analysis has great potential. Although many new strategies have been proposed for the application of SLIPS to droplet manipulation, the loss of lubricant is still an inevitable problem, and the realization of complex droplet guiding paths is also difficult. Therefore, more exploration will be essential.

## Summary and outlook

Slippery liquid-infused porous surfaces, as an emerging type of omniphobic surface, are conceptually different from superhydrophobic surfaces inspired by the lotus leaf effect. In imitation of the inner wall of the insect trap of the *Nepenthes* pitcher plant, a lubricant with low surface tension is infused into a porous substrate material to prepare a repellent surface containing a thin liquid layer. The surface not only has superhydrophobic performance including self-cleaning, anti-icing, and anticorrosion, but the injected lubricant also gives it unique pressure stability, self-healing capability, and extremely low contact angle hysteresis. In application, this slippery performance makes SLIPS more advantageous in anti-icing and anti-fouling. Since the lubricant layer is in direct contact with the repelled liquid instead of the solid surface, the lubricant can be adjusted to adapt to different environments and has fewer requirements for the type and micromorphology of the substrate. SLIPS can be constructed on most materials, including metals and metal alloys, nonmetallic materials, and porous polymers, which greatly expands its application range. However, there are still some problems for practical application. The incorporation of lubricants is two-sided. Although it adds excellent

characteristics to SLIPS, it also brings additional challenges. All the characteristics of the slippery liquid-infused porous surface are based on the stability of the liquid-infused system. Once the lubricant layer is worn out, function is lost. Therefore, overcoming lubricant loss is an important direction for future research. In medical applications, in addition to focusing on stability, we must also focus on the nontoxicity of lubricants. At present, it has been proven that some lubricants do not affect cell growth, including perfluorododecane (PFD), perfluoropolyether (PFPE), and silicone oil, and more biocompatible lubricants can be explored. In addition, most lubricants are fluorine-containing compounds which are harmful to the environment and do not conform to the scientific concept of sustainable development. Therefore, environmentally friendly lubricants must be the general trend. In brief, although there are still some shortcomings in practical applications that will require continuous improvement, SLIPS provides new ideas and new methods for solving the problems faced in many fields and has far-reaching research significance.

**Acknowledgements** This work was financially supported by the National Natural Science Foundation of China (No. 51735013)

**Author contributions** XZ was involved in conceptualization, writing—original draft, and visualization. ZG and WL helped in writing—review and editing. WL contributed to supervision.

## Declarations

**Conflict of interest** The authors declare that there is no conflict of interest.

**Ethical approval** This study does not contain any studies with human or animal subjects performed by any of the authors.

## References

- Barthlott W, Neinhuis C (1997) Purity of the sacred lotus, or escape from contamination in biological surfaces. *Planta* 202:1–8. <https://doi.org/10.1007/s004250050096>
- Sun T, Feng L, Gao X et al (2005) Bioinspired surfaces with special wettability. *Acc Chem Res* 38(8):644–652. <https://doi.org/10.1021/ar040224c>
- Gangadoo S, Chandra S, Power A et al (2016) Biomimetics for early stage biofouling prevention: templates from insect cuticles. *J Mater Chem B* 4:5747–5754. <https://doi.org/10.1039/C6TB01642A>
- Bhushan B, Jung YC (2011) Natural and biomimetic artificial surfaces for superhydrophobicity, self-cleaning, low adhesion, and drag reduction. *Prog Mater Sci* 56(1):1–108. <https://doi.org/10.1016/j.pmatsci.2010.04.003>
- Si Y, Zhu H, Chen L et al (2015) A multifunctional transparent superhydrophobic gel nanocoating with self-healing properties. *Chem Commun* 51:16794–16797. <https://doi.org/10.1039/C5CC06977G>
- Lu Y, Sathasivam S, Song J et al (2015) Robust self-cleaning surfaces that function when exposed to either air or oil. *Science* 347(6226):1132–1135. <https://doi.org/10.1126/science.aaa0946>
- Milles S, Soldera M, Kuntze T et al (2020) Characterization of self-cleaning properties on superhydrophobic aluminum surfaces fabricated by direct laser writing and direct laser interference patterning. *Appl Surf Sci* 525:146518. <https://doi.org/10.1016/j.apsusc.2020.146518>
- Bhushan B, Martin S (2018) Substrate-independent superliquiphobic coatings for water, oil, and surfactant repellency: an overview. *J Colloid Interf Sci* 526:90–105. <https://doi.org/10.1016/j.jcis.2018.04.103>
- Martin S, Brown PS, Bhushan B (2017) Fabrication techniques for bioinspired, mechanically-durable, superliquiphobic surfaces for water, oil, and surfactant repellency. *Adv Colloid Interf Sci* 241:1–23. <https://doi.org/10.1016/j.cis.2017.01.004>
- Nishimoto S, Bhushan B (2013) Bioinspired self-cleaning surfaces with superhydrophobicity, superoleophobicity, and superhydrophilicity. *RSC Adv* 3:671–690. <https://doi.org/10.1039/C2RA21260A>
- Fu JJ, Chen T, Wang MD et al (2013) Acid and alkaline dual stimuli-responsive mechanized hollow mesoporous silica nanoparticles as smart nanocontainers for intelligent anticorrosion coatings. *ACS Nano* 7(12):11397–11408. <https://doi.org/10.1021/nn4053233>
- Bhushan B, Multanen V (2019) Designing liquid repellent, icephobic and self-cleaning surfaces with high mechanical and chemical durability. *Phil Trans R Soc A* 377(2138):20180270. <https://doi.org/10.1098/rsta.2018.0270>
- Cremaldi J, Bhushan B (2018) Fabrication of bioinspired, self-cleaning superliquiphilic/phobic stainless steel using different pathways. *J Colloid Interf Sci* 518:284–297. <https://doi.org/10.1016/j.jcis.2018.02.034>
- Nanda D, Varshney P, Satapathy M et al (2017) Single step method to fabricate durable superliquiphobic coating on aluminum surface with self-cleaning and anti-fogging properties. *J Colloid Interf Sci* 507:397–409. <https://doi.org/10.1016/j.jcis.2017.08.022>
- Amini S, Kollé S, Petrone L (2017) Preventing mussel adhesion using lubricant-infused materials. *Science* 357(6352):668–673. <https://doi.org/10.1126/science.aai8977>
- Cameron SW, Smith-Palmer T, Peppou-Chapman S et al (2018) Marine antifouling behavior of lubricant-infused nanowrinkled polymeric surfaces. *ACS Appl Mater Interf* 10(4):4173–4182. <https://doi.org/10.1021/acsami.7b14736>
- Li H, Shkolyar E, Wang J et al (2020) SLIPS-LAB—a bioinspired bioanalysis system for metabolic evaluation of urinary stone disease. *Sci Adv* 6(21):eaba8535. <https://doi.org/10.1126/sciadv.aba8535>
- Epstein AK, Wong T, Belisle RA et al (2012) Liquid-infused structured surfaces with exceptional anti-biofouling performance. *PNAS* 109(33):13182–13187. <https://doi.org/10.1073/pnas.1201973109>
- Maccallum N, Howell C, Kim P et al (2015) Liquid-infused silicone as a biofouling-free medical material. *ACS Biomater Sci Eng* 1(1):43–51. <https://doi.org/10.1021/ab5000578>
- Badv M, Jaffer IH, Weitz JI et al (2017) An omniphobic lubricant-infused coating produced by chemical vapor deposition of hydrophobic organosilanes attenuates clotting on catheter surfaces. *Sci Rep* 7:11639. <https://doi.org/10.1038/s41598-017-12149-1>
- Goudie MJ, Pant J, Handa H (2017) Liquid-infused nitric oxide-releasing (LINORel) silicone for decreased fouling, thrombosis, and infection of medical devices. *Sci Rep* 7:13623. <https://doi.org/10.1038/s41598-017-14012-9>
- Manna U, Raman N, Welsh MA et al (2016) Slippery liquid-infused porous surfaces that prevent microbial surface fouling

- and kill non-adherent pathogens in surrounding media: a controlled release approach. *Adv Funct Mater* 26(21):3599–3611. <https://doi.org/10.1002/adfm.201505522>
23. Wong TS, Kang S, Tang S et al (2011) Bioinspired self-repairing slippery surfaces with pressure-stable omniphobicity. *Nature* 477(7365):443–447. <https://doi.org/10.1038/nature10447>
  24. Jung S, Tiwari M, Doan N et al (2012) Mechanism of super-cooled droplet freezing on surfaces. *Nat Commun* 3:615. <https://doi.org/10.1038/ncomms1630>
  25. Grace M, Gao L, Stephen Y et al (2019) Clinical potential of immobilized liquid interfaces: perspectives on biological interactions. *Trends Biotechnol* 37(3):268–280. <https://doi.org/10.1016/j.tibtech.2018.08.003>
  26. Young T (1805) An essay on the cohesion of fluids. *Phil. Trans R Soc* 95:65–87. <https://doi.org/10.1098/rstl.1805.0005>
  27. Liu J, Fang X, Zhu C et al (2020) Fabrication of superhydrophobic coatings for corrosion protection by electrodeposition: a comprehensive review. *Colloid Surf A Physicochem Eng Asp* 607:125498. <https://doi.org/10.1016/j.colsurfa.2020.125498>
  28. Villegas M, Zhang Y, Abu Jarad N et al (2019) Liquid-infused surfaces: a review of theory, design, and applications. *ACS Nano* 13(8):8517–8536. <https://doi.org/10.1021/acsnano.9b04129>
  29. Lee K, Kim YS, Shin K (2012) Hierarchically-structured artificial water-repellent leaf surfaces replicated from reusable anodized aluminum oxide. *Macromol Res* 20:762–767. <https://doi.org/10.1007/s13233-012-0111-5>
  30. Wenzel RN (1936) Resistance of solid surfaces to wetting by water. *Ind Eng Chem* 28(8):988–994. <https://doi.org/10.1021/ie50320a024>
  31. Valipour MN, Birjandi FC, Sargolzaei J (2014) Super-non-wettable surfaces: a review. *Colloid Surf A Physicochem Eng Aspects* 448:93–106. <https://doi.org/10.1016/j.colsurfa.2014.02.016>
  32. Yong J, Chen F, Yang Q et al (2017) Superoleophobic surfaces. *Chem Soc Rev* 46(14):4168–4217. <https://doi.org/10.1039/C6CS00751A>
  33. Cassie ABD, Baxter S (1944) Wettability of porous surfaces. *Trans Faraday Soc* 40:546–551. <https://doi.org/10.1039/TF9444000546>
  34. Bhushan B (2019) Lessons from nature for green science and technology: an overview and bioinspired superliquiphobic/philic surfaces. *Phil Trans R Soc A* 377(2138):20180274. <https://doi.org/10.1098/rsta.2018.0274>
  35. Gou X, Guo Z (2019) Surface topographies of biomimetic superamphiphobic materials: design criteria, fabrication and performance. *Adv Colloid Interf Sci* 269:87–121. <https://doi.org/10.1016/j.cis.2019.04.007>
  36. Shao Y, Zhao J, Fan Y et al (2020) Shape memory superhydrophobic surface with switchable transition between “Lotus Effect” to “Rose Petal Effect.” *Chem Eng J* 382:122989. <https://doi.org/10.1016/j.cej.2019.122989>
  37. Cao M, Guo D, Yu C et al (2016) Water-repellent properties of superhydrophobic and lubricant-infused “slippery” surfaces: a brief study on the functions and applications. *ACS Appl Mater Interf* 8(6):3615–3623. <https://doi.org/10.1021/acsmi.5b07881>
  38. Liu M, Wang S, Wei Z et al (2009) Bioinspired design of a superoleophobic and low adhesive water/solid interface. *Adv Mater* 21(6):665–669. <https://doi.org/10.1002/adma.200801782>
  39. Cai Y, Lin L, Xue Z et al (2014) Filefish-inspired surface design for anisotropic underwater oleophobicity. *Adv Funct Mater* 24(6):809–816. <https://doi.org/10.1002/adfm.201302034>
  40. Parker A, Lawrence C (2001) Water capture by a desert beetle. *Nature* 414:33–34. <https://doi.org/10.1038/35102108>
  41. Garrod RP, Harris LG, Schofield WCE et al (2007) Mimicking a stenocara beetle’s back for microcondensation using plasma-chemical patterned superhydrophobic-superhydrophilic surfaces. *Langmuir* 23(2):689–693. <https://doi.org/10.1021/la0610856>
  42. Hou Y, Yu M, Chen X et al (2015) Recurrent filmwise and dropwise condensation on a beetle mimetic surface. *ACS Nano* 9(1):71–81. <https://doi.org/10.1021/nn505716b>
  43. Holger F, Bohn WF (2004) Insect aquaplaning: *Nepenthes* pitcher plants capture prey with the peristome, a fully wettable water-lubricated anisotropic surface. *PNAS* 101(39):14138–14143. <https://doi.org/10.1073/pnas.0405885101>
  44. Wang P, Lu Z, Zhang D (2015) Slippery liquid-infused porous surfaces fabricated on aluminum as a barrier to corrosion induced by sulfate reducing bacteria. *Corros Sci* 93:159–166. <https://doi.org/10.1016/j.corsci.2015.01.015>
  45. Shi Z, Xiao Y, Qiu R et al (2017) A facile and mild route for fabricating slippery liquid-infused porous surface (SLIPS) on CuZn with corrosion resistance and self-healing properties. *Surf Coat Technol* 330:102–112. <https://doi.org/10.1016/j.surfcoat.2017.09.053>
  46. Barati Darband Gh, Aliofkhaezraei M, Khorsand S et al (2020) Science and engineering of superhydrophobic surfaces: review of corrosion resistance, chemical and mechanical stability. *Arab J Chem* 13(1):1763–1802. <https://doi.org/10.1016/j.arabjc.2018.01.013>
  47. Chen L, Guo Z, Liu W (2017) Outmatching superhydrophobicity: bio-inspired re-entrant curvature for mighty superamphiphobicity in air. *J Mater Chem A* 5:14480–14507. <https://doi.org/10.1039/C7TA03248J>
  48. Wang S, Liu K, Yao X et al (2015) Bioinspired surfaces with superwettability: new insight on theory, design, and applications. *Chem Rev* 115(16):8230–8293. <https://doi.org/10.1021/cr400083y>
  49. Kim P, Kreder MJ, Alvarenga J et al (2013) Hierarchical or not? Effect of the length scale and hierarchy of the surface roughness on omniphobicity of lubricant-infused substrates. *Nano Lett* 13(4):1793–1799. <https://doi.org/10.1021/nl4003969>
  50. Rykaczewski K, Paxson A, Staymates M et al (2014) Dropwise condensation of low surface tension fluids on omniphobic surfaces. *Sci Rep* 4:4158. <https://doi.org/10.1038/srep04158>
  51. Gryniov R, Bormashenko E, Whyman G et al (2016) Superoleophobic surfaces obtained via hierarchical metallic meshes. *Langmuir* 32(17):4134–4140. <https://doi.org/10.1021/acs.langmuir.6b00248>
  52. Starostin A, Valtsifer V, Strelnikov V et al (2014) Robust technique allowing the manufacture of superoleophobic (omniphobic) metallic surfaces. *Adv Eng Mater* 16(9):1127–1132. <https://doi.org/10.1002/adem.201300561>
  53. Ellinas K, Chatzipetrou M, Zergioti I et al (2015) Superamphiphobic polymeric surfaces sustaining ultrahigh impact pressures of aqueous high- and low-surface-tension mixtures, tested with laser-induced forward transfer of drops. *Adv Mater* 27(13):2231–2235. <https://doi.org/10.1002/adma.201405855>
  54. Boreyko JB, Polizos G, Datskos PG et al (2014) Air-stable droplet interface bilayers on oil-infused surfaces. *Proc Natl Acad Sci USA* 111(21):7588–7593. <https://doi.org/10.1073/pnas.1400381111>
  55. He W, Liu P, Jiang J et al (2018) Development of multifunctional liquid-infused materials by printing assisted functionalization on porous nanocomposites. *J Mater Chem A* 6:4199–4208. <https://doi.org/10.1039/C7TA10780C>
  56. Zhao H, Park KC, Law KY (2012) Effect of surface texturing on superoleophobicity, contact angle hysteresis, and “robustness.” *Langmuir* 28(42):14925–14934. <https://doi.org/10.1021/la302765t>
  57. Chen J, Long M, Peng S et al (2017) Superamphiphobic aluminum surfaces that maintain robust stability after undergoing severe chemical and physical damage. *N J Chem* 41(3):1334–1345. <https://doi.org/10.1039/C6NJ03696A>

58. Sun Y, Wang L, Gao Y et al (2015) Preparation of stable superamphiphobic surfaces on Ti-6Al-4V substrates by one-step anodization. *Appl Surf Sci* 324:825–830. <https://doi.org/10.1016/j.apsusc.2014.11.047>
59. Hao L, Yu S, Han X et al (2015) Design of submicron structures with superhydrophobic and oleophobic properties on zinc substrate. *Mater Des* 85:653–660. <https://doi.org/10.1016/j.matdes.2015.07.057>
60. Liu Y, Zhao L, Lin J et al (2019) Electrodeposited surfaces with reversibly switching interfacial properties. *Sci Adv* 5(11):eaax0380. <https://doi.org/10.1126/sciadv.aax0380>
61. Liu Q, Yang Y, Huang M et al (2015) Durability of a lubricant-infused electrospray silicon rubber surface as an anti-icing coating. *Appl Surf Sci* 346:68–76. <https://doi.org/10.1016/j.apsusc.2015.02.051>
62. Hou L, Wang N, Wu J et al (2018) Bioinspired superwettability electrospun micro/nanofibers and their applications. *Adv Funct Mater* 28:1801114. <https://doi.org/10.1002/adfm.201801114>
63. Lee MW, An S, Latthe SS et al (2013) Electrospun polystyrene nanofiber membrane with superhydrophobicity and superoleophilicity for selective separation of water and low viscous oil. *Appl Mater Interf* 5(21):10597–10604. <https://doi.org/10.1021/am404156k>
64. Doll K, Fadeeva E, Schaeske J et al (2017) Development of laser-structured liquid-infused titanium with strong biofilm-repellent properties. *ACS Appl Mater Interf* 9(11):9359–9368. <https://doi.org/10.1021/acsami.6b16159>
65. Doll K, Yang I, Fadeeva E et al (2019) Liquid-infused structured titanium surfaces: antiadhesive mechanism to repel streptococcus oralis biofilms. *ACS Appl Mater Interf* 11(26):23026–23038. <https://doi.org/10.1021/acsami.9b06817>
66. Hosseini A, Villegas M, Yang J et al (2018) Conductive electrochemically active lubricant-infused nanostructured surfaces attenuate coagulation and enable friction-less droplet manipulation. *Adv Mater Interf* 5:1800617. <https://doi.org/10.1002/admi.201800617>
67. Zouaghi S, Six T, Bellayer S et al (2017) Antifouling biomimetic liquid-infused stainless steel: application to dairy industrial processing. *ACS Appl Mater Interf* 9(31):26565–26573. <https://doi.org/10.1021/acsami.7b06709>
68. Ouyang Y, Zhao J, Qiu R et al (2020) Nanowall enclosed architecture infused by lubricant: a bio-inspired strategy for inhibiting bio-adhesion and bio-corrosion on stainless steel. *Surf Coat Technol* 381:125143. <https://doi.org/10.1016/j.surfcoat.2019.125143>
69. Ouyang Y, Zhao J, Qiu R et al (2019) Liquid infused surface based on hierarchical dendritic iron wire array: an exceptional barrier to prohibit biofouling and biocorrosion. *Prog Org Coat* 136:105216. <https://doi.org/10.1016/j.porgcoat.2019.105216>
70. Awad TS, Asker D, Hatton BD (2018) Food-safe modification of stainless steel food-processing surfaces to reduce bacterial biofilms. *ACS Appl Mater Interf* 10(27):22902–22912. <https://doi.org/10.1021/acsami.8b03788>
71. Ma Q, Wang W, Dong G (2019) Facile fabrication of biomimetic liquid-infused slippery surface on carbon steel and its self-cleaning, anti-corrosion, anti-frosting and tribological properties. *Colloid Surf A Physicochem Eng Asp* 577:17–26. <https://doi.org/10.1016/j.colsurfa.2019.05.008>
72. Sousa MFB, Loureiro HC, Bertran CA (2020) Anti-scaling performance of slippery liquid-infused porous surface (SLIPS) produced onto electrochemically-textured 1020 carbon steel. *Surf Coat Technol* 382:125160. <https://doi.org/10.1016/j.surfcoat.2019.125160>
73. Ouyang Y, Zhao J, Qiu R et al (2019) Biomimetics leading to liquid-infused surface based on vertical dendritic Co matrix: a barrier to inhibit bioadhesion and microbiologically induced corrosion. *Colloid Surf A: Physicochem Eng Asp* 583:124006. <https://doi.org/10.1016/j.colsurfa.2019.124006>
74. Liu C, Li Y, Lu C et al (2020) Robust slippery liquid-infused porous network surfaces for enhanced anti-icing/deicing performance. *ACS Appl Mater Interf* 12(22):25471–25477. <https://doi.org/10.1021/acsami.0c05954>
75. Jiang D, Xia X, Hou J et al (2019) A novel coating system with self-reparable slippery surface and active corrosion inhibition for reliable protection of Mg alloy. *Chem Eng J* 373:285–297. <https://doi.org/10.1016/j.cej.2019.05.046>
76. Subramanyam SB, Azimi G, Varanasi KK (2014) Designing lubricant-impregnated textured surfaces to resist scale formation. *Adv Mater Interf* 1:1300068. <https://doi.org/10.1002/admi.201300068>
77. Guo H, Fuchs P, Casdorff K et al (2017) Bio-inspired superhydrophobic and omniphobic wood surfaces. *Adv Mater Interf* 4:1600289. <https://doi.org/10.1002/admi.201600289>
78. Wang J, Lu Y, Chu Q et al (2020) Facile construction of superhydrophobic surfaces by coating fluoroalkylsilane/silica composite on a modified hierarchical structure of wood. *Polymers* 12(4):813. <https://doi.org/10.3390/polym12040813>
79. Vena A, Kolle S, Stafslie S et al (2020) Self-stratifying porous silicones with enhanced liquid infusion and protective skin layer for biofouling prevention. *Adv Mater Interf* 8:2000359. <https://doi.org/10.1002/admi.202000359>
80. Basu S, Hanh BM, Isaiah Chua JQ et al (2020) Green biolubricant infused slippery surfaces to combat marine biofouling. *J Colloid Interf Sci* 568:185–197. <https://doi.org/10.1016/j.jcis.2020.02.049>
81. Yong J, Chen F, Yang Q et al (2017) Nepenthes inspired design of self-repairing omniphobic slippery liquid infused porous surface (SLIPS) by femtosecond laser direct writing. *Adv Mater Interf* 4:1700552. <https://doi.org/10.1002/admi.201700552>
82. Manna U, Lynn DM (2015) Fabrication of liquid-infused surfaces using reactive polymer multilayers: principles for manipulating the behaviors and mobilities of aqueous fluids on slippery liquid interfaces. *Adv Mater* 27(19):3007–3012. <https://doi.org/10.1002/adma.201500893>
83. Agrawal P, Salomons TT, Chiriack DS et al (2019) Facile actuation of organic and aqueous droplets on slippery liquid-infused porous surfaces for the application of on-chip polymer synthesis and liquid-liquid extraction. *ACS Appl Mater Interf* 11(31):28327–28335. <https://doi.org/10.1021/acsami.9b08849> Error! Hyperlinkreferencenotvalid
84. Howell C, Vu TL, Johnson CP et al (2015) Stability of surface-immobilized lubricant interfaces under flow. *Chem Mater* 27(5):1792–1800. <https://doi.org/10.1021/cm504652g>
85. Sett S, Yan X, Barac G et al (2017) Lubricant-infused surfaces for low-surface-tension fluids: promise versus reality. *ACS Appl Mater Interf* 9(41):36400–36408. <https://doi.org/10.1021/acsami.7b10756>
86. Peppou-Chapman S, Hong JK, Waterhouse A et al (2020) Life and death of liquid-infused surfaces: a review on the choice, analysis and fate of the infused liquid layer. *Chem Soc Rev* 49(11):3688–3715. <https://doi.org/10.1039/D0CS00036A>
87. Tian X, Banerjee S, Gonzalez-Alfonzo I et al (2020) Suppressing evaporative loss in slippery liquid-infused porous surfaces (SLIPS) with self-suspended perfluorinated nanoparticles. *Langmuir* 36(19):5106–5111. <https://doi.org/10.1021/acs.langmuir.0c00160>
88. Rao Q, Zhang J, Zhan X et al (2020) UV-driven self-replenishing slippery surfaces with programmable droplet-guiding pathways. *J Mater Chem A* 8:2481–2489. <https://doi.org/10.1039/C9TA11723G>

89. Zhao H, Sun Q, Deng X et al (2018) Earthworm-inspired rough polymer coatings with self-replenishing lubrication for adaptive friction-reduction and antifouling surfaces. *Adv Mater* 30:1802141. <https://doi.org/10.1002/adma.201802141>
90. Zhang D, Xia Y, Chen X et al (2019) PDMS-infused poly(high internal phase emulsion) templates for the construction of slippery liquid-infused porous surfaces with self-cleaning and self-repairing properties. *Langmuir* 35(25):8276–8284. <https://doi.org/10.1021/acs.langmuir.9b01115>
91. Jing X, Guo Z (2019) Fabrication of biocompatible super stable lubricant-immobilized slippery surfaces by grafting a polydimethylsiloxane brush: excellent boiling water resistance, hot liquid repellency and long-term slippery stability. *Nanoscale* 11(18):8870–8881. <https://doi.org/10.1039/C9NR01556F>
92. Meuler AJ, McKinley GH, Cohen RE (2010) Exploiting topographical texture to impart icephobicity. *ACS Nano* 4:7048–7052. <https://doi.org/10.1021/nn103214q>
93. Kim P, Wong T-S, Alvarenga J et al (2012) Liquid-infused nanostructured surfaces with extreme anti-ice and anti-frost performance. *ACS Nano* 6(8):6569–6577. <https://doi.org/10.1021/nl302310q>
94. Vazirinasab E, Maghsoudi K, Jafari R et al (2020) A comparative study of the icephobic and self-cleaning properties of Teflon materials having different surface morphologies. *J Mater Process Technol* 276:116415. <https://doi.org/10.1016/j.jmatprotec.2019.116415>
95. Latthe SS, Sutar RS, Bhosale AK et al (2019) Recent developments in air-trapped superhydrophobic and liquid-infused slippery surfaces for anti-icing application. *Prog Org Coat* 137:105373. <https://doi.org/10.1016/j.porgcoat.2019.105373>
96. Zhao L, He L, Liang J et al (2020) Facile preparation of a slippery oil-infused polymer surface for robust icephobicity. *Prog Org Coat* 148:105849. <https://doi.org/10.1016/j.porgcoat.2020.105849>
97. Tourkine P, Merrer ML, Quere D (2009) Delayed freezing on water repellent materials. *Langmuir* 25(13):7214–7216. <https://doi.org/10.1021/la900929u>
98. Jung S, Dorrestijn M, Raps D et al (2011) Are superhydrophobic surfaces best for icephobicity? *Langmuir* 27(6):3059–3066. <https://doi.org/10.1021/la104762g>
99. Chen J, Liu J, He M et al (2012) Superhydrophobic surfaces cannot reduce ice adhesion. *Appl Phys Lett* 101:111603. <https://doi.org/10.1063/1.4752436>
100. Wilson PW, Lu W, Xu H et al (2013) Inhibition of ice nucleation by slippery liquid-infused porous surfaces (SLIPS). *Phys Chem Chem Phys* 15(2):581–585. <https://doi.org/10.1039/C2CP43586A>
101. Juuti P, Haapanen J, Stenroos C et al (2017) Achieving a slippery, liquid-infused porous surface with anti-icing properties by direct deposition of flame synthesized aerosol nanoparticles on a thermally fragile substrate. *Appl Phys Lett* 110:161603. <https://doi.org/10.1063/1.4981905>
102. Long Y, Yin X, Mu P et al (2020) Slippery liquid-infused porous surface (SLIPS) with superior liquid repellency, anti-corrosion, anti-icing and intensified durability for protecting substrates. *Chem Eng J* 401:126137. <https://doi.org/10.1016/j.cej.2020.126137>
103. Li J, Feng X, Liu B et al (2017) Polymer materials for prevention of postoperative adhesion. *Acta Biomater* 61:21–40. <https://doi.org/10.1016/j.actbio.2017.08.002>
104. Leslie DC, Waterhouse A, Berthet JB et al (2014) A bioinspired omniphobic surface coating on medical devices prevents thrombosis and biofouling. *Nat Biotechnol* 32(11):1134–1140. <https://doi.org/10.1038/nbt.3020>
105. Yuan S, Luan S, Yan S et al (2015) Facile fabrication of lubricant-infused wrinkling surface for preventing thrombus formation and infection. *ACS Appl Mater Interf* 7(34):19466–19473. <https://doi.org/10.1021/acsami.5b05865>
106. Badv M, Imani SM, Weitz JI et al (2018) Lubricant-infused surfaces with built-in functional biomolecules exhibit simultaneous repellency and tunable cell adhesion. *ACS Nano* 12(11):10890–10902. <https://doi.org/10.1021/acsnano.8b03938>
107. Howell C, Grinthal A, Sunny S et al (2018) Designing liquid-infused surfaces for medical applications: a review. *Adv Mater* 30(50):e1802724. <https://doi.org/10.1002/adma.201802724>
108. Zou M, Zhao X, Zhang X et al (2020) Bio-inspired multiple composite film with anisotropic surface wettability and adhesion for tissue repair. *Chem Eng J* 398:125563. <https://doi.org/10.1016/j.cej.2020.125563>
109. Beyzavi A, Nguyen N-T (2010) Programmable two-dimensional actuation of ferrofluid droplet using planar microcoils. *J Micro-mech Microeng* 20(1):015018. <https://doi.org/10.1088/0960-1317/20/1/015018>
110. Luo JT, Gerald NR, Guan JH et al (2017) Slippery liquid-infused porous surfaces and droplet transportation by surface acoustic waves. *Phys Rev Appl* 7:014017. <https://doi.org/10.1103/PhysRevApplied.7.014017>
111. Ting TH, Yap YF, Nguyen NT et al (2006) Thermally mediated breakup of drops in microchannels. *Appl Phys Lett* 89:234101. <https://doi.org/10.1063/1.2400200>
112. Gao W, Wang J, Zhang X et al (2020) Electric-tunable wettability on a paraffin-infused slippery pattern surface. *Chem Eng J* 381:122612. <https://doi.org/10.1016/j.cej.2019.122612>
113. Chen C, Huang Z, Jiao Y et al (2019) In situ reversible control between sliding and pinning for diverse liquids under ultra-low voltage. *ACS Nano* 13(5):5742–5752. <https://doi.org/10.1021/acsnano.9b01180>
114. Guo T, Che P, Heng L et al (2016) Anisotropic slippery surfaces: electric-driven smart control of a drop's slide. *Adv Mater* 28(32):6999–7007. <https://doi.org/10.1002/adma.201601239>
115. Hou G, Cao M, Yu C et al (2017) Foolproof method for fast and reversible switching of water-droplet adhesion by magnetic gradients. *ACS Appl Mater Interf* 9(27):23238–23245. <https://doi.org/10.1021/acsami.7b07409>